DEVELOPMENT AND CHARACTERIZATION OF GLASS CERAMIC FROM COCA-COLA GLASS BOTTLE AND MAGNESITE

BY

ASMA'U IBRAHIM GEBI

DEPARTMENT OF METALLURGICAL AND MATERIALS ENGINEERING,
FACULTY OF ENGINEERING,
AHMADU BELLO UNIVERSITY, ZARIA,
NIGERIA.

SEPTEMBER, 2015

DEVELOPMENT AND CHARACTERIZATION OF GLASS CERAMIC FROM COCA-COLA GLASS BOTTLE AND MAGNESITE

By

Asma'u Ibrahim GEBI, B ENG (ABU) 2010
MSc/Eng/1471/2011-2012

A DISSERTATION SUBMITTED TO THE SCHOOL OF POST GRADUATE STUDIES,
AHMADU BELLO UNIVERSITY, ZARIA

IN PARTIAL FULFILLMENT OF THE REQUIREMENTS FOR THE AWARD OF A
MASTER DEGREE IN METALLURGICAL AND MATERIALS ENGINEERING

DEPARTMENT OF METALLURGICAL AND MATERIALS ENGINEERING,
FACULTY OF ENGINEERING,
AHMADU BELLO UNIVERSITY, ZARIA
NIGERIA

SEPTEMBER, 2015

DECLARATION

I declare that the work in the dissertation titled 'DEVELOPMENT AND CHARACTERIZATION OF GLASS CERAMIC FROM COCA-COLA GLASS BOTTLE AND MAGNESITE' has been carried out by me in the Department of Metallurgical and Materials Engineering.

The information derived from the literature has been duly acknowledged in the text and a list of references provided.

No part of the dissertation was previously presented for another degree or diploma at this or any other Institution.

Gebi, Asma'u Ibrahim	______________________	**September, 2015**
Name of Student	**Signature**	**Date**

CERTIFICATION

This dissertation titled 'DEVELOPMENT AND CHARACTERIZATION OF GLASS CERAMIC FROM COCA-COLA GLASS BOTTLE AND MAGNESITE' by Asma'u Ibrahim GEBI meets the regulations governing the award of the degree of Master of Science of the Ahmadu Bello University, Zaria, and is approved for its contribution to knowledge and literary presentation.

_Prof. S. A. Yaro______________ ____________________ ________
Chairman, Supervisory Committee Signature Date

_Dr. M. Abdulwahab____________ ____________________ _________
Member, Supervisory Committee Signature Date

___Prof. S. A. Yaro___________ ____________________ ________
Head of Department Signature Date

Prof. K. Bala
------------------------------- ------------------------------ -------------
Dean, School of Postgraduate Studies Signature Date

ACKNOWLEDGEMENTS

All praise is due to almighty Allah for seeing me through this project. My thanks go to my able HOD and supervisor Prof S. A. Yaro, and second supervisor Dr. M. Abdulwahab for their tremendous patience, guidance, encouragement, support and understanding.

To all members of staff of the department, I appreciate your encouragement and support. I am grateful for the assistance provided by various laboratory managers, engineers and technicians who helped me with my research especially Ishaq Mahmood Ashaka cem, Malam Sulaiman M., Mr Danladi and others, I owe you immense thanks.

To all other flowers that gave me air, thank you very much I appreciate you all.

Finally I wish to express my gratitude to members of my family, for believing in me, supporting me and always being next to me in every step I choose to take. Special mention has to be made of my dearest Husband Umar Faruq Hassan, for literally ‘beating me into form’ to ensure that the work is brought to an end.

ABSTRACT

In a bid to address environmental challenges associated with the management of waste Coca cola glass bottle, this study sets out to develop glass ceramic materials using waste Coca cola glass bottles. Magnesite from Sakatsimta in Adamawa state and reagent grade chrome (coloring agent) were used to modify the composition of the coca cola glass bottle; x-ray fluorescence (XRF), x-ray diffraction (XRD) and thermo gravimetric analysis (TGA) were used to characterize the raw materials. Four batches GC-1= (Coca cola glass frit +1%Cr_2O_3), GC-2= (97% Coca cola glass frit+ 2%magnesite+1%Cr_2O_3), GC-3= (95% Coca cola glass frit+ 4%magnesite+1%Cr2O_3) and GC-4= (93%Coca cola glass frit+ 6%magnesite+ 1%Cr_2O_3) were formulated and prepared. TGA results were used as a guide in selection of three temperatures (700^0C, 750^0C and 800^0C) used for the study. Three particle sizes -106+75, -75+53, -53μm and 2hrs sintering time were used. The sinter crystallization route of glass ceramic production was adopted. Produced samples were characterized by x-ray diffraction (XRD) technique and scanning electron microscopy (SEM), the density, porosity, hardness and flexural strength of the resulting glass ceramics were also measured using Archimedes principle, ASTM C373, ASTM C348, ASTM C1327 respectively. The resulting glass ceramic materials composed mainly of wollastonite, diopside and anorthite phases depending on composition as revealed by XRD and SEM. The density of the samples increased with increasing sintering temperature and decreasing particle size while the porosity was minimal and decreased with increasing sintering temperature and decreasing particle size. The obtained glass ceramic materials possessed appreciable hardness and flexural strength with GC-3 and GC-4 having the best

combination of both properties. It is therefore recommended that both compositions be used were a good combination of the aforementioned property is required.

TABLE OF CONTENTS

Cover page	
Fly Leaf	
Title Page	i
Declaration	ii
Certification	iii
Acknowledgement	iv
Abstract	v
Table of Content	x
List of Figures	xiv
List of Tables	xv
List of Plates	xv
List of appendices	xvi
Abbreviations	xviii
CHAPTER ONE	
1.0 INTRODUCTION	1
1.1 Statement of research problem	4

1.2 Justification 5

1.3 Aim and Objectives 5

1.4 scope of the research 6

1.5 Contribution to Knowledge 6

2.0LITERATURE REVIEW

2.1 Ceramic materials 8

2.2 Classification of ceramic materials 8

2.3 Structure of ceramic materials 9

2.4 Advance Ceramics 9

2.5 Glass Ceramics 10

2.6 Ceramic Processing and Crystal Growth 12

2.7 Processing Routes for Glass-Ceramic Production 16

2.7.1 Conventional Method (Two-Stage) 16

2.7.2 Modified Conventional Method (Single-Stage) 16

2.7.3 Petrurgic Method 17

2.7.4 Powder Methods 17

2.7.5 Sol-Gel Precursor Glass 19

2.8 Glass Ceramic Composition Systems Relevant To the Study 19

2.8.1 SiO_2-Al_2O_3-CaO (Wollastonite) 19

2.8.2 SiO_2-$A1_2O_3$-MgO (Cordierite, Enstatite) 19

2.8.2.1 Cordierite Glass-Ceramics 19

2.8.2.2 Enstatite Glass-Ceramic 20

2.9 Sintering 21

2.9.1 Overview of Sintering Theory 22

2.9.2 Mechanisms of Sintering 23

2.9.3 Factors Affecting Sintering 24

2.10 Advantages of Glass Ceramics 24

2.11 Application of Glass ceramics.

3.0 EXPERIMENTAL PROCEDURE

3.1 Materials and Equipment 26

3.1.1 Materials 26

3.1.2 Equipment 26

3.2 Raw material characterization 26

3.2.1 X-ray fluorescence (XRF) 26

3.2.2 X-ray diffraction (XRD) 27

3.2.3 Thermo gravimetric analysis (TGA) 27

3.3 Sample Preparation 28

3.3.1 Batch Formulation and Preparation 28

3.4 Characterization of the glass ceramic Samples 31

3.4.2. X-ray diffraction (XRD) 31

3.4.3 Scanning Electron Microscope (SEM) 31

3.5 Tests for Physical and Mechanical Properties 31

3.5.1 Density 32

3.5.2 Porosity 32

3.5.3 Flexural Strength 32

3.5.4 Hardness 33

4.0 RESULTS AND DISCUSSION

4.1 Results 35

4.2 Discussion of results 36

4.2.1 X ray Diffraction and X ray Fluorescence of Raw Materials 36

4.2.2 Thermo gravimetric analysis (TGA) 38

4.2.3X-ray diffraction (XRD) 40

4.2.4Scanning Electron Microscope 51

4.2.5 Density 55

4.2.6 Porosity 56

4.2.7 Flexural Strength 62

4.2.8 Hardness 62

5.0 CONCLUSION AND RECOMMENDATIONS

5.1 Conclusion 63

5.2 Recommendations 64

REFERENCES 66

List of Figures

Figure4.1: XRD pattern of magnesite 36

Figure4.2: TGA curve of glass sample. 37

Figure 4.3: X-ray diffraction patterns for: a) GC-1(-53µm, 700^{o}C), b) GC-1(-53µm, 800^{o}C), c) GC-2 (-75+53µm, 700^{o}C), d) GC-2(-75+53µm, 700^{o}C) 38

Figure 4.4: X-ray diffraction patterns for: a) GC-3(-75+53µm, 800^{o}C), b) GC-3(-75+53µm, 750^{o}C), c) GC-4 (-75+53µm, 800^{o}C), d) GC-4(-53µm, 750^{o}C) 39

Figure4.5: Variation of density and porosity with different conditions of particle size and temperature of GC-1 samples 48

Figure4.6: Variation of density and porosity with different conditions of particle size and temperature for GC-2 samples. 49

Figure4.7: Variation of density and porosity with different conditions of particle size and temperature for GC-3 samples. 50

Figure4.8: Variation of density and porosity with different conditions of particle size and temperature for GC-4 samples 51

Figure4.9: Variation of hardness and flexural strength with different conditions of particle size and temperature for GC-1samples 52

Figure4.10: Variation of hardness and flexural strength with different conditions of particle size and temperature for GC-2samples 53

Figure4.11: Variation of hardness and flexural strength with different conditions of particle size and temperature for GC-3samples 54

Figure4.12: Variation of hardness and flexural strength with different conditions of particle size (µm) and temperature (^{O}C) for GC-4sample 55

List of Tables

Table3.1: Raw material composition of batches 29

Table3.2: calculated chemical composition of batches. 30

Table4.1: Chemical composition of coca cola glass bottle and magnesite 34

List of Plates

Plate I: SEM/EDS micrographs of GC-1(-53µm, 700^{o}C), with fine texture of tiny wollastonite in residual glass matrix. 40

Plate II: SEM/EDS micrographs of GC-1(-53µm, 800^{o}C): a) x5000 b) x10000, with fibrous growth of wollastonite in residual glass matrix 41

Plate III: SEM/EDS SEM/EDS micrographs of GC-2(-75+53µm, 700^{o}C): a) x5000 b) x10000 with fibrous growth of tiny diopside and wollastonite with appearance of tiny spherulites of anorthite 42

Plate IV: SEM/EDS micrographs of GC-2(-75+53µm, 800^{o}C): a) x5000 b) x10000, showing fibrous growth of tiny diopside and wollastonite with appearance of tiny spherulites of anorthite 43

Plate V: SEM/EDS micrographs of GC-3(-75+53µm, 800^{o}C) a) x5000 b) x10000: showing fibrous growth of tiny diopside and wollastonite with appearance of tiny spherulites of anorthite 44

Plate VI: SEM/EDS micrographs of GC-3(-75+53µm, 750^{o}C) a) x5000 b) x10000: showing fibrous growth of tiny diopside and wollastonite with appearance of tiny spherulites of anorthite 45

Plate VII: SEM/EDS micrographs of GC-4(-75+53µm, 800^{o}C) a) x5000 b) x10000: showing fibrous growth of tiny diopside and wollastonite with appearance of tiny spherulites of anorthite 46

Plate VIII: SEM/EDS micrographs of GC-4(-53µm, 750^{o}C) a) x5000 b) x10000: showing fibrous growth of tiny diopside and wollastonite with appearance of tiny spherulites of anorthite 47

List of Appendices

Table A1: variation of density and porosity with different conditions of particle size and 68
Table A2: variation of density and porosity with different conditions of particle size and 68
Table A3: variation of density and porosity with different conditions of particle size and temperature for GC-3 samples. 69
Table A4: variation of density and porosity with different conditions of particle size and temperature for GC-4 samples. 70
Table B1: variation of hardness and flexural strength with different conditions of particle size and temperature for GC-1 samples 71
Table B2: variation of hardness and flexural strength with different conditions of particle size and temperature for GC-2 samples 71
Table B3: variation of hardness and flexural strength with different conditions of particle size and temperature for GC-3 samples 72
Table B4: variation of hardness and flexural strength with different conditions of particle size and temperature for GC-3 samples 73
Table C1: XRD Mineral Card of a) GC-1(-53µm, 700^{o}C) 74

Table C2: XRD Mineral Card for GC-1(-53µm, 800^{o}C) 75
Table C3: XRD Mineral Card for GC-2 (-75+53µm, 700^{o}C) 76
Table C4: XRD Mineral Card for GC-2(-75+53µm, 700^{o}C) 77
Table C5: XRD Mineral card for GC-3(-75+53µm, 800^{o}C) 78

Table C6: XRD Mineral card for GC-3(-75+53µm, 750^{o}C) 79

Table C7: XRD Mineral card for GC-4 (-75+53µm, 800^{o}C) 80

Table Cf8: XRD Mineral card for GC-4(-53µm, 750^{o}C) 81

Abbreviations

1. XRF X ray Fluorescence
2. XRD X ray Diffraction
3. TGA Thermo Gravimetric Analysis
4. SEM Scanning Electron Microscopy

CHAPTER ONE

1.0 INTRODUCTION

The chronology of the human race from inception has been predicated on one material or the other in the form of tools or simple machine for usage. Historically the development and advancement of societies have been intimately tied to the members' ability to produce and manipulate materials to provide their needs. In fact early civilizations have been designated by the level of their materials development (Stone age, Bronze age, Iron age) (Callister, 2007). Modern science and technology constantly require new materials with special properties to achieve breathtaking innovations.This development centers on the improvement of scientific and technological fabrication and working procedures by rendering them faster, economically more viable and better in quality, at the same time new materials are introduced to improve general quality of life. Among the entire new materials: glass ceramic materials play a very special role as they offer the possibility of combining the special properties of conventional sintered ceramics with the distinctive characteristic of glass (Holland and Beall, 2002).

Glass ceramic, a family of polycrystalline materials produced by the controlled crystallization of glasses-generally induced by nucleating additives constitutes an essential part of modern living, since they are used as cookware through critical but familiar uses in dental restoration to the even more critical use in missile radomes. They are yet to find complete replacement in the face of stiff competitions from synthetic products such as plastics and other lightweight materials. The several advantages offered by glass over other materials, which have served to reinforce its competitiveness over a long period of use spanning several centuries include exceptional chemical durability, multifaceted optical properties and complete recycling capability in an era of heightened environmental consciousness (Ali, 2008).

Glass ceramics are normally produced from specially formulated compositions-which usually contain a nucleating agent. They are melted and shaped into articles of desired geometry and then cooled to glass (Khater *et* al, 2012). After that the glass articles are subjected to heat treatments to initiate the growth of crystals in situ. Commonly such heat treatment process is carried out in two steps, at the temperature within or slightly above the transformation range, to develop nuclei in the glass, and then followed by another higher temperature treatment to enhance the growth of crystals on the formed nuclei (Locsei, 1962). Thus by precipitating crystal phases in the base glass new exceptional characteristics are achieved. Among these is the machinability of glass ceramics resulting from mica crystallization and the minimum thermal expansion of chinaware, kitchen hotplates or scientific telescope as a result of β-quartz and β-spodumene crystallization (Ali, 2008).

Glass-ceramics are normally obtained by a controlled crystallization of suitable glasses. Internal or external nucleation is promoted to develop micro-heterogeneities from which crystallization can subsequently begin. As a result, the amorphous reservoir of the parent glass transforms into a uniform microcrystalline ceramic. The composition of the crystalline phases and the crystallite sizes define the properties of the final material. Therefore, the major components and the composition of the parent glass are selected to ensure precipitation of crystals that provide desired properties on a glass-ceramic (Holland

and Beall, 2002). In the case of internally nucleated glass-ceramics, the use of high specific surface glass-powders will act as uniformly scattered nuclei and no addition of a special nucleating agent is required. Subsequently densification of the glass-powder compact must take place prior to devitrification. This sequence of events starting near the end of the sintering stage comes before crystallization starts which allows dense materials to be obtained (Siligardi *et* al., 2000).

The sintering process has been an important tool in the fabrication of various materials into useful articles. For thousands of years, it was used to create tools and implements out of naturally occurring ceramic materials. Today, it is used to manufacture a wide range of products for consumers, electronics, transportation and biomedical systems and applications, e.g., rocket nozzles, ultrasonic transducers, automobile engines, semiconductor packaging substrate, and dental implants. For ceramic materials including many glasses, sintering remains the most important, if not the only viable fabrication route. It is also used for other materials such as refractory metals and alloys where melting is not a practical method because of the extreme temperature required. Unlike melting, the material(s) need not be transformed into the liquid state for consolidation and densification to take place and it can be done at temperatures hundreds of degrees below the melting point. The article essentially retains its shape, albeit with reduced dimensions. Advances in technology require multi-component structures, an area where sintering is a suitable process. The use of finer starting glass powders gives glass ceramic materials with highly homogeneous microstructures and smoother surfaces. The glossy aspect is also retained. Simultaneous improvement of functional properties like the mechanical resistance to abrasion and flexural stresses make these materials very attractive for several applications (e.g. the textile industry) (Calata, 2005).

Other relevant aspects of the development of glass ceramic materials include environmental and economic issues. The use of natural (and cheap) raw materials and their adaptability for fabrication by different techniques (injection molding, isostatic pressing, etc.) help to produce cost competitive and multi-shaped devices, therefore the use of cheap and abundant raw materials as glass batch constituents is logically preferred. The choice of primary raw materials for the production of glass ceramic is very important. Different varieties of natural rocks and various sedimentary rock mixtures are being increasingly used for the production of glass ceramic materials. Igneous rocks such as granites, basalts and nepheline syenite are used successfully in the production of glass ceramic (Khater *et* al., 2012).

1.1 Statement of research problem

Recently, industrial and domestic wastes and their potential impacts on humans and environment during disposal and management have been identified as one of the most challenging problems facing society (Khater *et* al., 2012). The Nigerian bottling company in its effort to address environmental and social challenges is working to reduce the environmental impacts of its packaging at every stage of its lifecycle. To achieve this, it has considered many factors such as the weight and volume of solid wastes generated, the energy consumed in manufacturing and delivering various types of packaging, the airborne and waterborne pollutants emitted during manufacturing, and dozens of other factors.

PET (Polyethylene terephthalate) was concluded to be the fastest growing packaging option in the industry. The preference for pet bottles leaves us with a number of waste glass bottles that have been produced over the years thereby adding to the existing environmental challenges of waste management and control.

1.2 Justification

Traditionally, most garbage (domestic waste) is buried in landfills or disposed in incinerators. But landfills are closing down all over Nigeria and incineration is a poor alternative. Even with pollution controls, incinerators are a large source of air pollution in most communities in Nigeria. Additionally, incinerators produce millions of tons of toxic ash, which still have to go to landfills. This shows that it has severe impact on the environment and there is need to promote any process that will enable its reduction. For these reasons, one could, as a first option, submit the waste to a high temperature sintering process in order to convert it into a more environmentally friendly product (glass ceramic) as in this study.

1.3 Aim and Objectives

The aim of this research work is to develop and characterize a glass ceramic material by sinter crystallization of waste Coca Cola glass bottles and magnesite. The specific objectives include:

- Characterize coca cola bottle using x-ray fluorescence (XRF) and magnesite using x-ray diffraction (XRD) and (XRF),

- Investigate the thermal behaviors of the glass bottle frits using thermo gravimetric analysis (TGA) and prepare condition of thermal treatment for the glass ceramic,
- Identify the phases present in the glass ceramics using x-ray diffraction (XRD),
- Investigate the physical and mechanical properties of the glass ceramic,
- Study the microstructure of the glass ceramic material using scanning electron microscopy (SEM).

1.4 Scope of the Research

The scope of this research covered production of the glass ceramic by sinter crystallization, use of TGA, XRF, XRD, and SEM to characterize the material. Physical (density and porosity) and mechanical (hardness and flexural strength) properties were also studied.

1.5 Contribution to Knowledge

To the best of my knowledge no research work has been carried out on the development and characterization of glass ceramic using coca cola glass bottle and magnesite. Consequently, successful completion of this research has provided information on the possibility of producing a glass ceramic from coca cola glass bottle and magnesite, furthermore the different phases and microstructural morphology of the various compositions investigated have been established.

CHAPTER TWO

2.0 LITERATURE REVIEW

2.1 Ceramic Materials

Ceramic materials are complex compounds containing both metallic and non-metallic elements. Typically, ceramics are very hard, brittle, high melting point materials with low electrical and thermal conductivity, good chemical and thermal stability, and high compressive strength (Durrani *et al*., 2012). Ceramics are of tremendous interest primarily because of their wide range of applications in high temperature environments; they are also extensively used in fuel technology (Koshiro *et al*., 1995), oxygen sensor (Ciacchi, *et al*., 1994), magnets ceramics (Valenzuela, 2005) , all electronic equipments including Integrated-chips, capacitors and digital alarms (Miller and Miller (2002)), telecommunication (Bhargava, 2005), abrasives, ceramic crystal-glass (Carter and Norton, 2007). Ceramic insulators are widely used in the electrical power transmission system (Chowdhury, 2010), ceramic superconductors (David and Zoitos, 1992) and pharmaceuticals industries (Rice and W. Rice, 2002) etc**.**

2.2 Classification of Ceramic Materials

Ceramic materials can be classified into four main groups (Rajendran, 2004):

i. The amorphous ceramics, which are generally referred to as "glasses",

ii. Crystalline ceramics**,** which are single phase materials like alumina, or mixtures of such materials,

iii. Bonded ceramics**,** where individual crystals are bonded together by a glassy matrix, such as clay products,

iv. Cements**,** these are crystalline, and also amorphous materials.

2.3 Structure of Ceramic Materials

The structures of ceramics fall into two main groups:

• Simple crystal structures: containing ionic or covalent bonds, or a mixture of the two. Examples are magnesium oxide, which is an ionic compound with cubic structure, and silicon carbide, with covalent bonds and a tetrahedral structure like diamond. Alumina has a close packed hexagonal structure, with a mixture of covalent and ionic bonds, with one-third of the potential aluminum sites vacant in order to suit the valency requirements of the two elements (Mostaghaci, 1996).

• Complex silicate structure**s:** The majority of ceramic materials, which are derived from clay, sand or cement, contain the silicon in the form of silicates. The arrangements involve both chains of silicate ions $(SiO_4)_2$–, double chains and links in sheet form.

2.4 Advance Ceramics

In advance ceramic, extremely pure microscopic raw materials are used, with strict control of compositions and manufacturing conditions, in order to achieve a more uniform microstructure. Interest in modern ceramic continues to grow because these materials have a unique set of properties which no other family of materials can match. These include high hardness, heat resistance, ability to withstand corrosive atmosphere, resistance to abrasion, ability to sustain compressive loads at elevated temperatures, and an inexpensive and abundant availability of raw materials. Except for brittleness, ceramics stand out well against metals and plastics and can be applied as thermal barrier coatings to protect metal structures, wearing surfaces, or as integral components by themselves. These new ceramics are called either "new ceramics or fine ceramics" or frequently called "high-performance ceramics" as described elsewhere (Durrani *et al*., 2012).

2.5 Glass Ceramics

Glass-ceramics are ceramic materials formed through the controlled nucleation and crystallization of glass. Glasses are melted, fabricated to shape, and thermally converted to a predominantly crystalline ceramic. The basis of controlled internal crystallization lies in efficient nucleation that allows the development of fine, randomly oriented grains generally without voids, micro cracks, or other porosity. The glass-ceramic process, therefore, is basically a simple thermal process as illustrated in Figure 2.1.

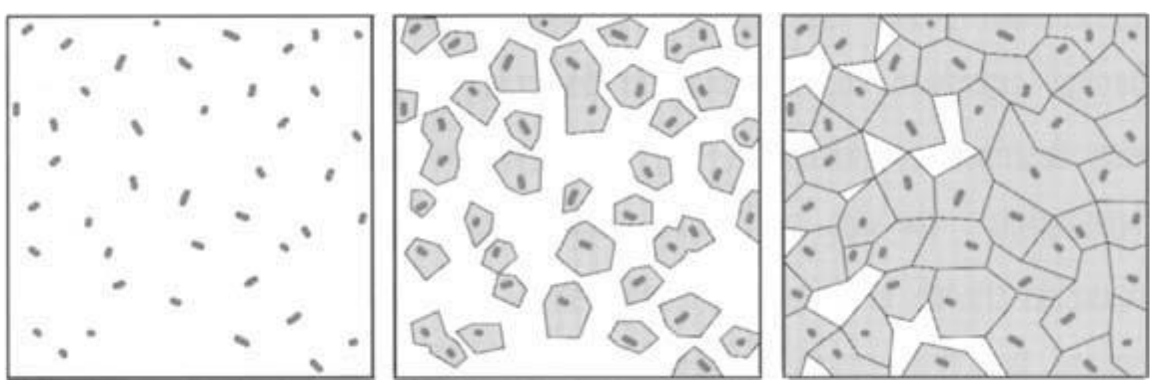

Figure 2.1: The glass-ceramic process; (a) nuclei formation, (b) crystal growth on nuclei, (c) glass-ceramic microstructure.

(Source: Hölland and Beall, 2002).

Glass ceramic materials are fine grained polycrystalline solid containing residual glass phase formed by melting of glass and forming into products by the way of controlled crystallization of a specially formulated glass (Shackelford and Doremus, 2008). These are primarily silicates containing oxides such as Al_2O_3, TiO_2, LiO_2, and others. In amorphous form, the glasses are transparent. Glasses can be made to transform into a polycrystalline state by a suitable heat-treatment process. A nucleating agent, such as TiO_2, is added to begin the `nucleation of ceramic crystals. The product is called glass ceramic.

Glass ceramics are members of the ceramic family and an important electroceramic type were first investigated in the 1950s by Stookey at Corning Glass (Durrani *et al*, 2005**).** They are extensively exploited as electrical insulators in electronic industries and have a wide variety of technological applications such as microelectronic substrates and packaging, optically transparent components, biomedical implants, catalytic supports, membranes and sensors, as well as for the matrix of composite materials (Durrani *et al*., 2012). In addition, they have been used in protection layers, sewing-thread in textile industry, ceramic tiles and also are developed into a very promising substrate material of computer hard disk (Novaes *et al*., 1994)**.**

The universal glass ceramics are Lithia-alumina-silica (Li_2O-ZrO_2-SiO_2-Al_2O_3, LZSA) systems that have zero thermal expansion co-efficient, and hence no thermal shock problem (Montedo *et al*., 2009). The majorities of commercial glass ceramic products are formed by highly automated glass forming processes and are converted to a crystalline product by the proper heat treatment. Glass-ceramics can be prepared through powder processing methods, in which glass frits are sintered and crystallized. The range of potential glass-ceramic compositions is therefore particularly wide, requiring only the ability to form a glass and control its crystallization. Glass-ceramics can provide advantages over conventional glass or ceramic materials, by combining the simplicity and flexibility of forming and inspection of glass with improved and often unique properties in glass ceramic. They possess highly uniform microstructures, with crystal sizes (<10mm), they generally are at least 50% crystalline by volume and often are >90% crystalline. Glass-ceramics are also called pyrocerams, vitrocerams, devitrocerams, sitalls, slag ceramics, melt-formed ceramics, and devitrifying frits (Ali, 2008).

2.6 Ceramic Processing and Crystal Growth

Glass-ceramic materials are produced by means of either bulk or powder processing methods. In these methods, glass-ceramic products are melted and fabricated to shape in the glass state. Most used forming methods are rolling, pressing, spinning, casting, and blowing. The product is then crystallized using a heat treatment, designed for that material. This process, known as ceramic processing, usually comprises of a low temperature hold to induce nucleation, followed by a higher temperature hold to promote crystallization and growth of the primary phase. Because crystallization occurs at high viscosity, product shapes are typically preserved with little or no shrinkage (1-3%) or deformation during the ceramming. Nucleation generally begins with phase separation, whereby an amorphous, homogeneous glass unadulterates into two immiscible phases of different compositions. Controlled devitrification is only possible for certain glass compositions and generally takes place in two stages: formation of submicroscopic nuclei, and their growth into macroscopic crystals. These two stages are called nucleation and crystal growth (Hölland,*et al*., 2002).

Nucleation occurs when a small piece of solid forms from the liquid. The solid must achieve a certain minimum critical radius (r_c) before it is stable. Growth of crystal occurs as atoms from the liquid are attached to the tiny solid until no liquid remains. Devitrification means the formation of crystals on or inside of amorphous glass, typically due to a delayed cooling cycle. The presence of local crystalline inclusions supports the glass and makes it more flexible, reducing the presence and severity of micro-cracks and acting as crack stoppers. The heat treatment that supports the growth of these native crystals during the glass formation is called ceramming and it is a two-step process (Durrani *et al*., 2012).

Ceramming is a controlled crystallization of the glass that results in the formation of tiny crystals that are uniformly distributed throughout the body of the glass structure. The size of the crystals, as well as the number and rate of growth is measured by the time and temperature of the ceramming heat treatment. There are two stages of ceramming process; crystal nucleation and crystal growth. Each stage takes place because the glass body is retained at an exact temperature for a definite length of time (Cattell, 2006).

Crystals have a propensity to develop in a mixture of glass when it is held at a specific temperature, called the crystal nucleation temperature. This means that when held at the crystal nucleation temperature, multiple seed crystals begin to grow throughout the glass body. The longer the glass is kept at this temperature, the more seed crystals will be formed. Ideally, a glass ceramic will be strongest when there are a very large number of small crystals distributed uniformly all over its mass. Once a seed crystal forms, it will also begin to grow larger at this temperature, but somewhat slowly. If the temperature of the glass body is held at the crystal nucleation temperature for a very long time, a very large number of crystals of broadly varying size will form. The initial seeds will be largest, while the crystals that started to grow later will be the smallest (Durrani *et al*., 2012).

To better control the art of the finished product, the ideal glass ceramic will have crystals of a small and uniform size. Any form of devitrification in a glass structure will produce one degree of opacity. Large crystals are flat to make the glass opaque, while small crystals uniformly scattered throughout the structure have less of an impact on the optical qualities of the finished product. Thus it is of advantage to keep the temperature at the point of maximum seeding for a finite length of time in order to allow several tiny seed crystals to nucleate, and then to stop the nucleation process and support the ones that have formed to grow to appropriate size (Durrani *et al*., 2005).

The glass ceramic materials with tailor made properties can be fabricated by controlling nucleation and crystal growth process. Although some glass compositions are self-nucleating, generally some nucleating agents are added to the batch to promote phase separation and internal nucleation. These melt homogeneously into the glass, but promote very fine phase separation on reheating. The isolated phase, which can be a metal, titanate, zirconate, phosphate, sulfide, or halide, is structurally incompatible with the host glass and is usually highly unstable as a glass (Durrani *et al*., 2012).

Nucleation is followed by higher temperature treatments to promote crystallization and development of the desired microstructure. Most commercial glass-ceramic products are formed by highly mechanized glass-forming processes and converted to a crystalline product by proper heat treatment (Durrani *et al*., 2012).

Glass-ceramic materials have been prepared through powder processing in which glass frits are sintered and then crystallized. The range of potential glass-ceramic compositions is therefore extremely broad, requiring only the ability to form a glass and control its crystallization. The production of glass-ceramics from powder, using conventional ceramic processes such as spraying, slip-casting, or extrusion, extends the range of possible glass-ceramic compositions by taking advantage of surface crystallization. In these materials, the surfaces of the glass grains serve as the nucleating sites for the crystal phases. The glass composition and processing conditions are selected such that the glass softens, proceeding to crystallization and undergoes viscous sintering to full density just before the crystallization process is completed. Given these conditions, the final crystalline microstructure is basically the same as that produced from the bulk process (Durrani *et al*., 2012).

The precursor glass powders may be produced by various methods, the simplest being the milling of quenched glass to an average particle size of 3-15mm. Sol-gel processesin which highly uniform, ultrafine amorphous particles are grown in a chemical solution, may be preferable for certain applications (Yuan, *et al*., 2010). Such devitrifying frits are employed significantly as sealing frits for bonding glasses, ceramics, and metals. Other applications include co-fired multilayer substrates for electronic packaging, matrices for fiber-reinforced composite materials, refractory cements and corrosion-resistant coatings.

2.7 Processing Routes for Glass-Ceramic Production

2.7.1 Conventional Method (Two-Stage)

The conventional method for producing a glass-ceramic is to devitrify a glass by a two-stage heat treatment. The first stage is a low temperature heat treatment at a temperature that gives a high nucleation rate thus forming a high density of nuclei throughout the interior of the glass. A high density of nuclei is important as it leads to a desirable microstructure consisting of a large number of small crystals. The second stage is a higher temperature heat treatment at around temperature to produce growth of the nuclei at a reasonable rate.

The parent glass may be shaped prior to crystallization employing any of the well-established, traditional glass shaping methods such as casting and forming or more special methods such as extrusion (Atkinson, 1975).

2.7.2 Modified Conventional Method (Single-Stage)

The reason for the two-stage heat treatment of the glass is a consequence of the limited overlap between the nucleation and growth rate curves. If there is extensive overlap of the rate curves then nucleation and growth can take place during a single-stage heat treatment at the same temperature. The rate curves, particularly the nucleation rate curve, is sensitive to composition and hence by optimising the glass composition it is, in some cases, possible to obtain the necessary overlap. By judicious choice of nucleating agents, this was first achieved for the glass-ceramic system known as "Silceram" (Rawlings *et al*, 1997).

2.7.3 Petrurgic Method

Rawlings *et* al., (1997) found with "Silceram" that it made little difference whether the glass was heated up to nucleation and crystallization temperature ($T_{NG)}$ from room temperature or the molten glass was cooled to $T_{NG.}$ This led to the development of the production of certain glass-ceramics by a controlled, usually very slow, cooling of the parent glass from the molten state without a hold at an intermediate temperature. With this method, referred to in the recent literature as the petrurgic method, both nucleation and crystal growth can take place during the cooling (Francis *et al*., 2002). Both the modified conventional (single-stage) and the petrurgic methods are more economical than the conventional method (two-stage).

2.7.4 Powder Methods

The shaping by cold-compacting a powder followed by a high temperature heat treatment to sinter the compact is a common route for the fabrication of ceramics and it has been employed for glass-ceramic production (Hing et al., 1997). As there are limitations on the size and shape of components that may be cold compacted, and also considering the high cost of producing the powder, this method is only used if an obvious benefit is identified. It is more attractive to sinter a parent glass powder, which sinters by a viscous flow mechanism at lower temperatures (Scherer, 1977). It is important to consider the rates of viscous flow sintering and crystallization and the interaction of these processes. According to Bocaccini et al.,(1996) and Zanotto et al., (2001) if crystallization is too rapid the resulting high degree of crystallinity will hinder the low temperature sintering leading to an unacceptable amount of porosity . On the other hand, if sintering is fully completed before crystallization, then the final product is unlikely to differ significantly from those fabricated by other methods. With appropriate rates it is possible in some cases to fabricate a dense glass-ceramics by a sintering process in which both densification and crystallization take place simultaneously at the same temperature. Optimization of composition and sintering temperature can lead to different microstructures, and even different crystalline phases, compared to those from the conventional method, and hence different properties of the product. Pressure assisted densification methods such as hot pressing and hipping have also been successfully applied for the production of glass-ceramics from powders.

Although these methods give improved products exhibiting near full densification, they are more expensive than cold pressing.

Powder technology facilitates the production of dispersion reinforced glass-ceramic matrix composites (Bocaccini *et al*., 2001). Fabrication of these particle-reinforced composites involves intimately mixing the powdered parent glass with the reinforcement in the required proportions. The mixture is then shaped, sintered and crystallized. Hard and rigid inclusions used as reinforcement hinder the sintering process. The production of continuous fibre reinforced glass-ceramics is more complex and requires dedicated apparatus (Bocaccini, 2002). For both particulate- and fiber-reinforced glass-ceramics densification is usually carried out by hot pressing and a final heat treatment is required to achieve crystallization of the glass matrix (Rawlings *et* al., 1997).

2.7.5 Sol-Gel Precursor Glass

So far only glasses produced from the molten state have been considered but in the last decades there has been considerable interest in using sol-gel and colloidal techniques to obtain the precursor glass in either powder or bulk form. Thus all the methods for glass-ceramic production discussed previously may be used with glass produced by this route (Rawlings *et* al., 1997).

2.8 Glass Ceramic Composition Systems Relevant To the Study

2.8.1 SiO_2-Al_2O_3-CaO (Wollastonite)

The base glasses of this system are particularly suitable for producing glass-ceramics according to the mechanism of controlled surface crystallization. Conventional volume nucleation agents, such as TiO, and ZrO,, are used in the process. Glass-ceramics with a wollastonite main crystal phase have been made from these base glasses according to the mechanism above. Glass-ceramics of this type demonstrate special optical effects and other favorable properties. These materials are produced on a large scale and used as cladding in the building industry (Beall *et* al., 2002).

2.8.2 SiO_2-$A1_2O_3$-MgO (Cordierite, Enstatite)

2.8.2.1 Cordierite Glass-Ceramics

Glass-ceramics with a primary crystal phase of cordierite, $Mg_2Al_4Si_5O_{18}$, are of great commercial importance. The first glass-ceramics of this type were developed at the Corning Glass Works (Beall, 1992). Subsequently, other glass-ceramics of this basic type were developed. Cordierite glass-ceramics are distinguished for their special properties such as high mechanical strength, excellent dielectric properties, good thermal stability, and thermal shock resistance.

The nucleation and crystallization process of this cordierite glass-ceramic material was the subject of an international research project of the Technical Committee 7 of ICG (international Commission on Glass). The results of this project demonstrated that the crystallization of a powdered base glass with the composition of $Mg_2Al_4Si_{11}O_{30}$, takes place to form a P-quartz solid solution as the primary crystal phase, according to the mechanism of surface nucleation and crystallization. Nucleation takes place at the surface of the base-glass grains. Furthermore, special structural strains prefer the process of surface nucleation (Beall *et* al., 2002). .

2.8.2.2 Enstatite Glass-Ceramics

Beall in 1991 successfully developed glass-ceramics featuring an enstatite MgSiO, primary crystal phase in the tertiary SiO_2-$A1_2O_3$,-MgO system with small amounts of $A1_2O_3$. This crystal phase demonstrated very interesting properties during cooling of the glass-ceramics. It also exhibited martensitic transformation, which contributed to the toughening of the final product. The stoichiometric composition of enstatite, however, did not permit the formation of a stable base glass. Therefore, it was necessary to develop special glass compositions that would allow controlled crystallization into enstatite.

Three different mechanisms and types of processing were used by Echeverria and Beall (1991) to develop enstatite-type glass-ceramics:

- bulk nucleation and crystallization of monolithic base glasses by using nucleating substances
- surface nucleation mechanism with devitrified glass frits, which did not contain nucleating substances
- Sol-gel route for developing ceramic specimens consisting of 100% enstatite.

2.9 Sintering

Sintering is the most important step in powder processing because it is at this stage that the material is subjected to very high temperatures, causing the particles to form bonds that are needed to hold the mass together. Sintering occurs by atomic diffusion at high temperatures in processes that are stimulated by high temperatures (Kucynski *et al*., 1967). Substantial particle rearrangement and consolidation may occur initially, especially in loosely packed bodies (Richerson, 1992). The transport mechanisms that subsequently follow will depend on the type of material being sintered (Calata, 2005).

Amorphous materials generally sinter by viscous flow, which has been extensively studied by numerous investigators (Scherer, 1992). On the other hand, polycrystalline materials sinter by one or more mechanisms occurring singly or in parallel, depending on the materials system and sintering conditions (Rahaman, 2003). This makes it difficult to isolate the mechanisms involved and adds to the complexity of the sintering process. In general, bulk transport mechanisms such as volume diffusion, grain boundary diffusion, plastic flow, and viscous flow result in shrinkage or densification while surface transport does not. However, surface transport is recognized to be important in inter particle neck growth and the sintering of some covalent solids and low-stability ceramics (Calata, 2005).

2.9.1 Overview of Sintering Theory

Sintering is usually classified into several types based on the mechanisms that are thought to be responsible for shrinkage or densification. Sintering that proceeds mainly by solid-state diffusion falls under solid state sinterin*g*. Polycrystalline materials usually sinter by this process. On the other hand, amorphous materials sinter by viscous flow and are thus considered to undergo viscous sintering. Another type of sintering that makes use of a transient second phase that exists as a liquid at the sintering temperature is known as liquid phase sintering (Kwon, 1991). The liquid phase under the right conditions can provide a path for rapid transport and, therefore, rapid sintering. Finally, processes that make use of an externally applied pressure to enhance densification are classified under pressure sintering.

The entire sintering process is generally considered to occur in three stages (German, 1991). The stages are as follows:

(i) Initial stage, (ii) intermediate stage, (iii) and final stage. There is no clear-cut distinction between the stages since the processes that are associated with each stage tend to overlap each other. However, some generalizations can be made to distinguish one stage from the next. In the initial stage, particles can rearrange by rotating and sliding into more stable positions in response to the sintering forces. This contributes to shrinkage and an overall increase in density. During particle rearrangement, there is an increase in inter particle contact, enabling the formation of necks between particles. Neck formation and growth can take place by diffusion, vapor transport, plastic flow, or viscous flow. The initial stage is assumed to last until a neck radius of around 0.4 to 0.5 of the particle radius is attained (Calata, 2005).

The intermediate stage is considered to begin when the pores have attained their equilibrium shapes as dictated by surface and interfacial energies. Because the density remains low at this point, the pores are still continuous or interconnected. Densification is assumed to take place by the reduction in cross section of the pores. Eventually, pores become unstable and are pinched off from each other, leading to the final stage of sintering. Of the three stages, the intermediate stage covers the majority of the sintering process. The final stage covers the elimination of the isolated pores until the theoretical density is reached. This stage is also characterized by grain growth in which the larger grains tend to increase in size at the expense of the smaller grains. The extent of grain growth is dependent on both the material and the sintering condition (Calata, 2005).

2.9.2 Mechanisms of Sintering

Polycrystalline materials generally sinter by diffusion processes while amorphous materials by viscous flow. The driving force for all these mechanisms is the tendency of the material to reduce its chemical potential or energy. This is accomplished by material transport from regions of high energy to regions of lower energy. Surfaces, interfaces and grain boundaries have associated energies that depend on surface or boundary curvature. By eliminating or minimizing these surfaces or by reducing their curvature, the overall energy of the material is reduced. There are at least six different mechanisms of sintering in polycrystalline materials and only volume diffusion of matter from the grain boundaries or from dislocations in the neck region can produce densification. The other mechanisms, though, cannot be ignored because they can reduce the neck curvature and reduce the driving force and densification rate (Calata, 2005).

2.9.3 Factors Affecting Sintering

The most important factors involved during sintering process are "process variables" (temperature, time and furnace atmosphere), "materials variables" (particle size, shape and structure), green density and dimensional changes. Varieties of sintering methods are available for sintering the ceramic compacts i.e., standard pressure sintering, reaction-sintering, hot pressing, post-reaction sintering, recrystallization sintering, atmospheric pressure sintering, ultra-high-pressure sintering, chemical vapor deposition (CVD) and isostatic hot pressing (HIP) (Durrani et *al*. 2012).

2.10 Advantages of Glass Ceramics

Glass-ceramics have, in principle, several advantages.

• They can be mass produced by any glass-forming technique.

• It is possible to design their nanostructure or microstructure for a given application.

• They have zero or very low porosity.

• It is possible for them to combine a variety of desired properties, an example is combining very low thermal expansion coefficient with transparency in the visible wavelength range for cooking ware. Another is combining very high strength and toughness with translucency, biocompatibility, chemical durability and relatively low hardness for dental applications.

2.11 Application of Glass ceramics.

Glass-ceramic materials have found applications in many fields such as:

- Aerospace e.g. in radomes.
- Medicine e.g. in dental restoration and implants.
- Optical e.g. telescope mirrors, integrated lens array etc.
- Electrical and electronics e.g. insulators, electronic packaging etc.
- Construction/Architecture e.g. tiles, cladding etc.

CHAPTER THREE

3.0 EXPERIMENTAL PROCEDURE

3.1 Materials and Equipment

3.1.1 Materials

Materials used in this research work are; coca cola glass bottle, magnesite from Sakasimta Adamawa State, distilled water, chrome.

3.1.2 Equipment

The following machines and equipment were used in this research: weighing balance, ball mill, measuring cylinder, spring balance, hydraulic press, crucible furnace, universal materials testing machine, Thermo gravimetric analysis (TGA), X-ray fluorescence (XRF), X-ray diffraction (XRD), Scanning electron microscopy (SEM), and Vickers micro hardness testing machine.

3.2 Raw material characterization

3.2.1 X-ray fluorescence (XRF)

The chemical composition of the coca cola glass frits and magnesite were determined using XRF machine. Raw material samples were ground to less than 60µm, 1.0g was weighed into a clean dry fusion crucible, and 8.0g of flux was added and thoroughly mixed. 1.0 ml of 25% LiBr solution was added to the mixture using 1 ml pipette (the sample was not mixed after adding LiBr). The crucible was placed on the fusion machine crucible holder. The start button was pressed and held for 10 sec and released. The machine was automatically ignited and the fusion process was carried out by the machine. At the end of the process the machine indicated “Fusion successful”. The bead was labelled while still in the mould on the outer surface and the disc remover was used to transfer it into a paper wallet and the bead was ran on an XRF program “Reference curve”.

3.2.2 X-ray diffraction (XRD)

The magnesite sample was prepared for XRD analysis using a zero background sample holder. They were analyzed with a PANanalytical Empyrean diffractometer with PIXcel detector and fixed slits with Fe filtered Co-Kα radiation. The phases were identified using X’Per Highscore plus software and quantified using the Rietveld method.

3.2.3 Thermo gravimetric analysis (TGA)

The thermal behavior of the fine powdered (45-75 μm) glass sample was examined using a PERKINELMER TG-DTA16. The powdered glass was heated in Pt.-holder with another one containing Al_2O_3 as a reference material. A uniform heating rate of 30°C/ /min was adopted from 30-1000°C. Data were recorded using a computer- driven data acquisition system. The results obtained were used as a guide for determining the required heat treatment temperatures applied to induce crystallization of the glasses.

3.4 Sample Preparation

3.3.1 Batch Formulation and Preparation

In the light of the chemical analysis of coca cola bottle, it was decided to modify the composition in order to make it more suitable for obtaining glass-ceramic materials. Coca cola glass bottle, magnesite and chrome (coloring agent) were used as starting materials in batch preparations of the glass ceramics. Four batches graded GC-1, GC-2, GC-3, GC-4 were used for the study. The corresponding nominal and calculated compositions (from XRF result) of the batches are given in tables 3.1 and 3.2 respectively. Three size fractions -106 +75, -75 +53 and -53 µm, 2hrs sintering time and three temperatures 700^0C, 750^0C and 800^0C were used. Samples were designated as G_{MPT} where M= 0,1,2,3 for 0,2,4,6% magnesite respectively, P= 1, 2, 3 for -106+75, -75+53, -53µm size fractions respectively, and T= 1,2,3 for 700, 750 and 800^oC respectively , the magnesite was calcined at 400^0C for 2 hour; and the components of each batch were accurately weighed and properly mixed, 5M PVA was used as binder and samples were prepared in the ratio of 98.5 % material and 1.5% binder, 324 rectangular bar(61x16x5mm) samples, 9 samples for each set of conditions of M,P and T were prepared based on conventional powder methods for producing ceramics i.e. milling, weighing and mixing, granulating, weighing, pressing and sintering(sinter crystallization).

Table3.1: Raw material composition of batches

Batch	Composition
GC-1	99% Coca cola glass frit +1%Cr_2O_3
GC-2	97% Coca cola glass frit+ 2%magnesite+1%Cr_2O_3
GC-3	95% Coca cola glass frit+ 4%magnesite+1%Cr_2O_3
GC-4	93%Coca cola glass frit+ 6%magnesite+ 1%Cr_2O_3

Table3.2: calculated chemical composition of batches.

OXIDES	GC-1	GC-2	GC-3	GC-4
SiO2	67.40	66.40	65.40	66.70
Na2O	13.02	12.80	12.57	12.8
Al2O3	1.97	1.96	1.94	2.0
MgO	0.44	1.24	2.03	2.94
P2O5	0.04	0.04	0.04	0.04
SO3	0.4	0.4	0.4	0.4
CL	0.02	0.02	0.02	0.02
K20	0.77	0.77	0.76	0.78
CaO	13.9	14.35	14.81	13.87
TiO2	0.13	0.13	0.13	0.13
Cr2O3	1.02	1.02	1.03	1.06
MnO	0.008	0.008	0.008	0.009
Fe2O3	0.72	0.73	0.73	0.76
ZnO	0.008	0.008	0.008	0.009
Rb2O	0.004	0.004	0.004	0.004
SrO	0.09	0.09	0.09	0.09
ZrO2	0.03	0.03	0.03	0.03
PbO	0.01	0.01	0.01	0.01
Mn2O5	-	0.0004	0.001	0.001

3.4 **Characterization of the glass ceramic Samples.**

3.4.1. X-ray diffraction (XRD)

The identification of crystals precipitating in the course of crystallization was conducted by X-ray diffraction analysis of the powdered samples. The samples were prepared using a back loading preparation method. The samples were analysed using P Analytical X'Pert Pro powder diffractometer with X'Celerator detector and variable divergence and receiving slits set at 10mm, with Fe filtered and Co-Kα radiation.

3.4.2 Scanning Electron Microscopy (SEM)

Microstructural features of sintered samples were observed using SEM. Polished sections were put onto aluminum stud, dried in air and then loaded into the SEM to examine the morphology and elemental chemistry of the crystalline phases. The SEM used was a JEOL 5900 with a tungsten wire filament.

3.5 Tests for Physical and Mechanical Properties.

The following physical and mechanical properties were determined;

3.5.1 Density

Density of 36 samples was determined by Archimedes principle. The mass (M) of the samples was obtained using a digital weighing balance and the volume (V) with a measuring cylinder, the Corresponding densities (ρ) was calculated from;

$$\rho = \frac{M}{V} \qquad \text{3.1}$$

3.5.2 Porosity

Porosity of 36 samples was determined in accordance with standard procedure ASTM-C373. Samples were weighed using a spring balance to obtain the dry weight (D), they were each immersed in boiling water for one hour and a spring balance was used to take weight of saturated sample in air (Suspended Weight (A)), the weight of saturated sample in water (Soaked Weight (W)) was taken, the sample was removed and the porosity (P) was calculated from; (Soaked Weight - Dry Weight) x 100 / (Soaked Weight – Suspended Weight)

$$P = \frac{W-D}{W-A} \times 100\% \qquad \text{3.2}$$

3.5.3 Flexural Strength

The 3 point bend test (ASTM- C348) on a universal materials testing machine was used to determine the flexural strength of 108 samples. Samples were placed on two supporting pins set at 40mm apart and a third loading pin was lowered from above at a constant rate until sample failure. The load at failure and deflections was noted and the flexural strength was calculated from eqn 3.3. Three samples were used for each condition.

Flexural stress σ_f was calculated from;

$$\sigma_f = \frac{3FL}{2bd^2} \quad \text{……………………………………………………………………}3.3$$

Where:

F= applied load

L= length

b= thickness

d=height of beam

3.5.4 Hardness

Vickers micro-hardness of 36 samples was measured according to ASTM-C1327; indentation technique using Vickers diamond pyramid indenter on the micro hardness tester was used. The measurement was done on the surface by applying 300g load for 15 sec. Three Vickers measurement readings were taken for each sample and the average was recorded.

CHAPTER FOUR

4.0 RESULTS AND DISCUSSION

4.1 Results

The results obtained from the experiments are presented in table 4.1, figures 4.1-4.12, and plates' I-VIII

Table4.1: Chemical composition of coca cola glass bottle and magnesite

OXIDES	COCA COLA BOTTLE (%)	MAGNESITE (%)
SiO_2	68.07	8.12
Na_2O	13.15	0.10
Al_2O_3	1.99	1.10
MgO	0.45	39.90
P_2O_5	0.04	0.02
SO_3	0.41	0.03
CL	0.02	-
K_2O	0.78	0.28
CaO	14.04	3.45
TiO_2	0.13	0.10

Cr_2O_3	0.02	0.002
MnO	0.01	-
Fe_2O_3	0.73	0.74
ZnO	0.01	-
Rb_2O	0.005	-
SrO	0.09	0.015
ZrO_2	0.03	-
PbO	0.014	-
Mn_2O_5	-	0.03
LOI	-	46.113

4.2 **Discussion of Results**

4.2.1 X ray Diffraction and X ray Fluorescence of Raw Materials

Table 4.1 and figure 4.1 shows result of XRF and XRD analysis of coca cola glass frits and magnesite. XRF analysis of coca cola glass bottle revealed that it belongs to SiO_2- CaO-Na_2O base glass composition system. Magnesite contained 39.90% MgO alongside other oxides according to XRF while XRD confirmed that it contains 96.15% magnesite, 2.02% quartz and 1.83% dolomite.

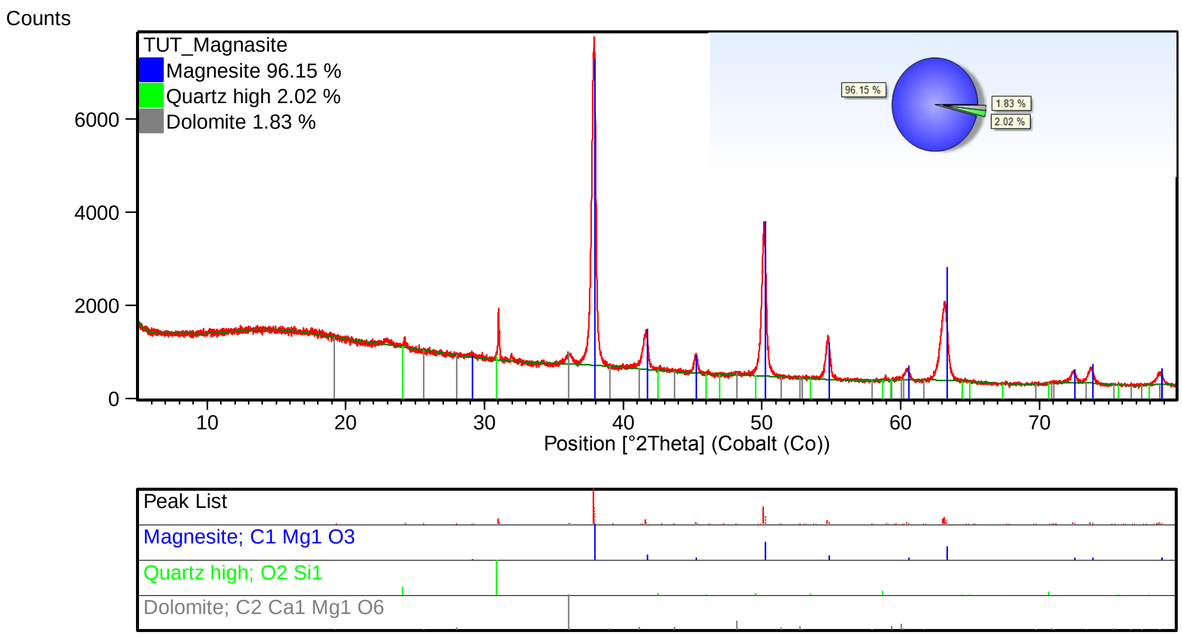

Figure 4.1.: XRD pattern of magnesite

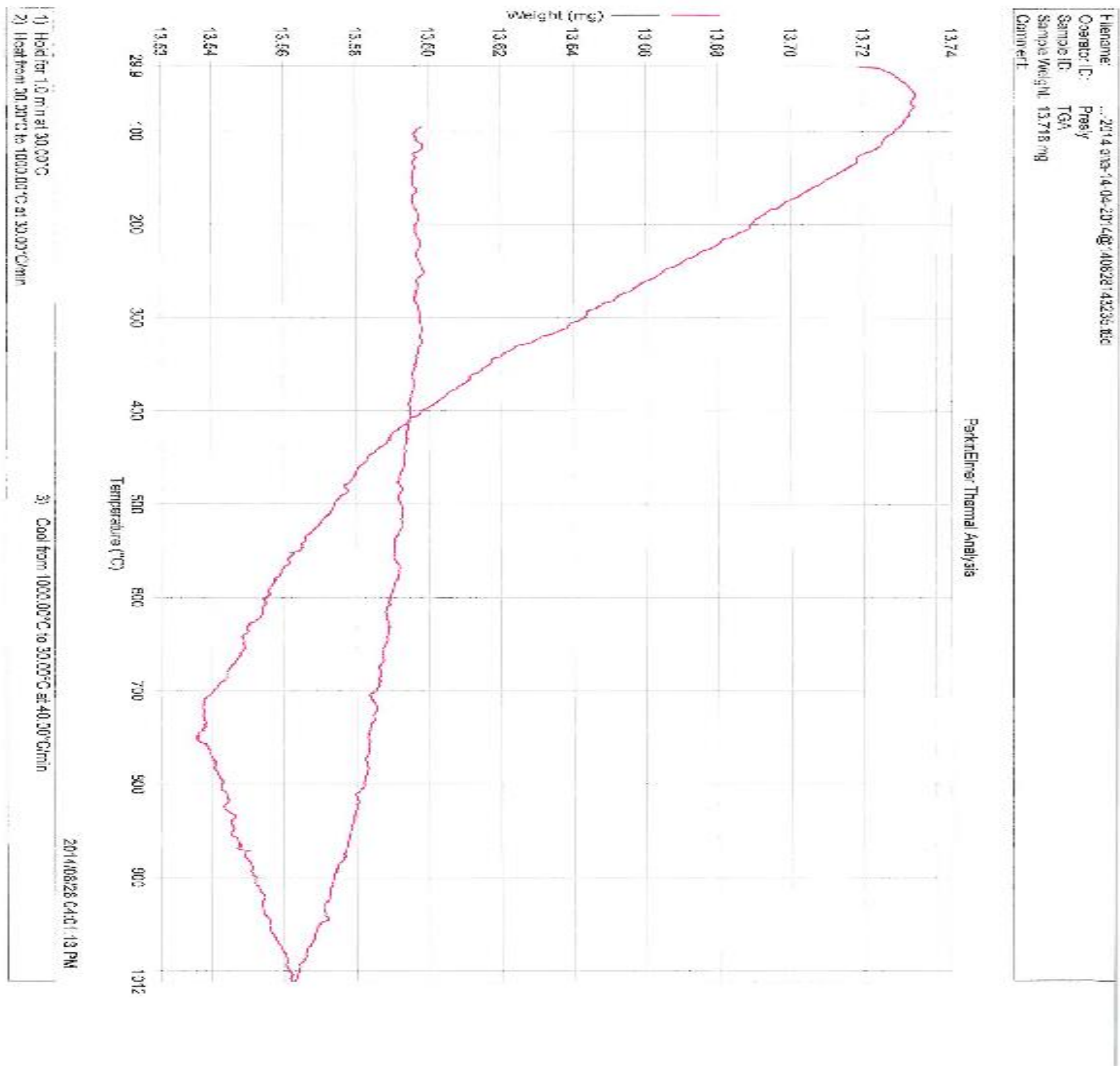

Figure 4.2: TGA curve of glass sample.

4.2.2 Thermo Gravimetric Analysis (TGA)

The TGA analysis is the proper method to determine the optimal stabilization temperature (Durrani *et al*., 2012). Thermal analysis TGA/DTA of coca cola glass bottle was done in the temperature range of 30-1000^{O}C in order to find the crystallization temperature of different crystalline phases as shown in Figure4.2. The total weight loss was observed after heating up to 750°C. Since the specimen was not fully dried, some physically bound water was present at the surface and in micro pores, which caused a subsequent loss of mass at the lowest temperature range, i.e., 50-400°C. This process is endothermic, which is connected with decomposition of water vapors. Between 400-700°C the weight loss was slow and steady, which probably is connected to glass transition/transformation, and from 700-750 °C the weight loss was constant due to the onset of sintering/nucleation. The nucleation temperature of the crystal is a strong function of the heating rate as found by Durrani *et*.al. (2012) it was observed that increasing the heating rate shifted the nucleation temperature to a higher value.

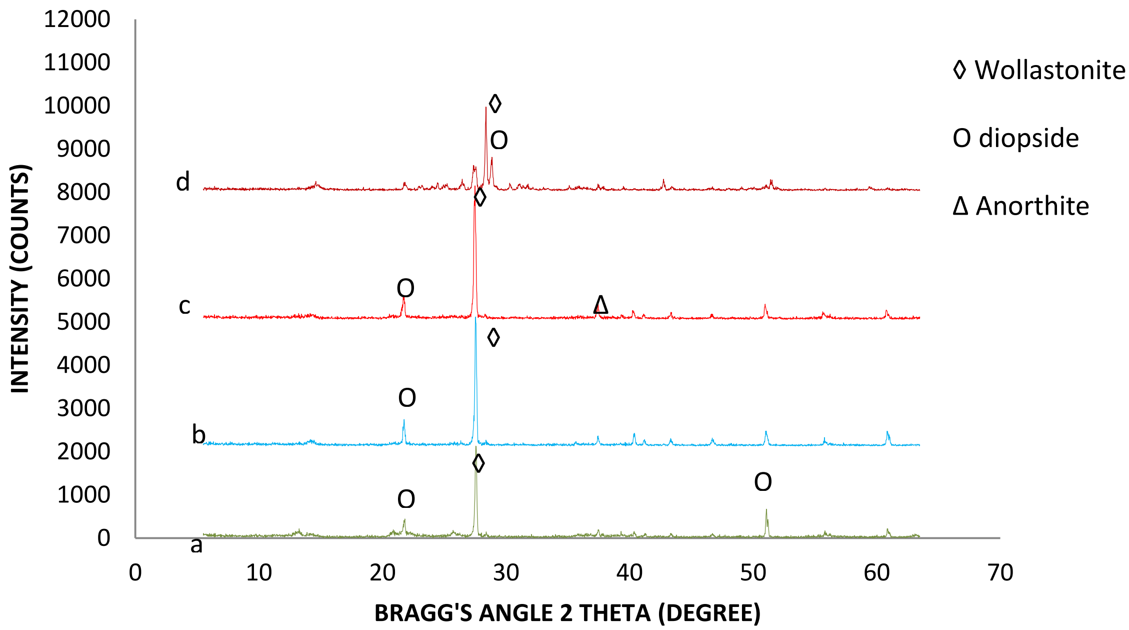

Figure 4.3: X-ray diffraction patterns for: a) GC-1(-53µm, 700°C), b) GC-1(-53µm, 800°C), c) GC-2 (-75+53µm, 700°C), d) GC-2(-75+53µm, 700°C)

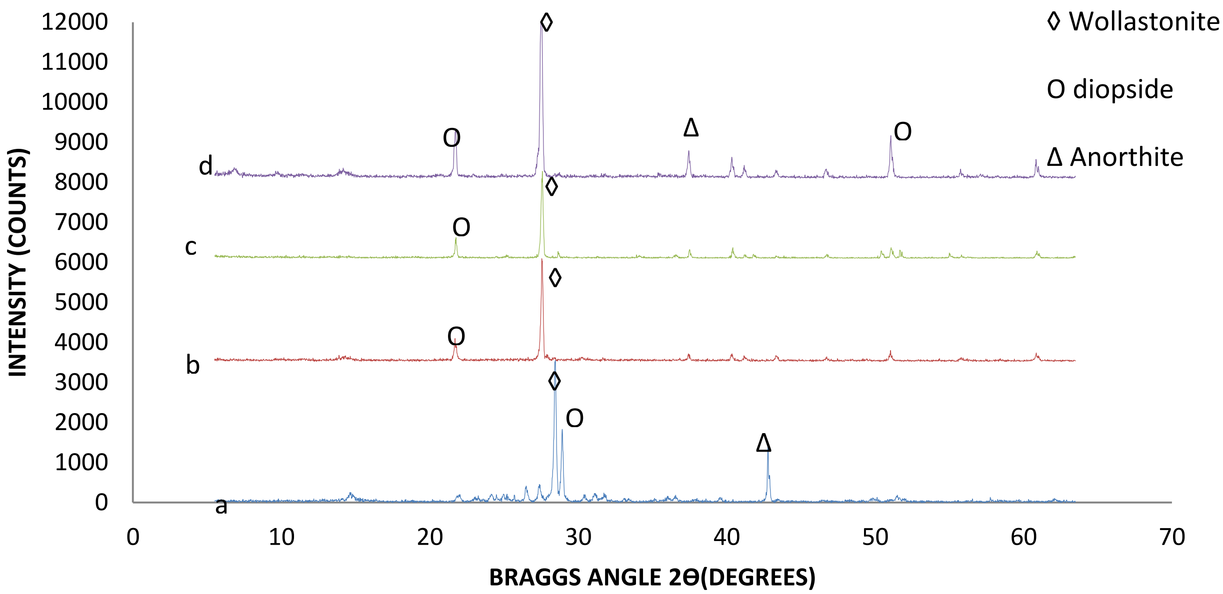

Figure 4.4: X-ray diffraction patterns for: a) GC-3(-75+53µm, 800^{o}C), b) GC-3(-75+53µm, 750^{o}C), c) GC-4 (-75+53µm, 800^{o}C), d) GC-4(-53µm, 750^{o}C)

4.2.3 X-ray Diffraction (XRD)

XRD analyses of samples GC-1, GC-2, GC-3 and GC-4 are shown in Figures 4.3 and 4.4. After sintering the appearance of wollastonite ($CaSiO_3$), diopside ($Ca,Mg(SiO_3)_2$) and weak anorthite ($CaAl_2Si_2O_8$) peaks can be seen. XRD results of glass ceramic compacts heat-treated suggest consecutive transformation of the parent glass into crystalline phases. Fig.4.2 shows the evolution of the GC-1 sample. The degree of crystallinity of formed phases and the composition of the residual glass changed with temperature evolution. The X-ray pattern of the GC-1 sample obtained at 700^{o}C is still basically composed of an amorphous glassy phase and a few intensity peaks of wollastonite ($CaSiO_3$) are observed. A further temperature increase to 800^oC enhances the intensity of the wollastonite peaks. The X-ray pattern of the GC-2 sample obtained at 700^oC is still basically composed of an amorphous glassy phase and a few intensity peaks of wollastonite ($CaSiO_3$) were observed as well as weakly defined new phases of monoclinic diopside ($CaMgSi_2O_6$) and anorthite. It seems that diopside and anorthite peaks were more pronounced in the sample with higher magnesite content (Figure4.4). X-ray diffraction showed that diopside, weak anorthite and wollastonite were the main crys talline phases developed in the investigated glasses. Their portion depended on base composition. In the sample GC-1 wollastonite ($CaSiO_3$) phase was crystallised. In the samples GC-2 to GC-4 the diopside and weak anorthite were developed better, especially in GC-3 and GC-4. Increase in the intensity of their lines was noticed. The increased intensities of diopside diffraction lines and their slight shift to higher 2θ values indicated a solid solution character.

The probable sequence of events during glass powder heat-treatment was as follows: (i) near the glass transition temperature (Tg), the parent glass fine particles acted as uniformly scattered nuclei; chrome also precipitated from the glass and formed nucleation points for the crystallization of wollastonite and diopside, and consequently induced the crystallization of the glasses. (ii) Further heating led to an increase in the viscosity of the batch and promoted densification by viscous coalescence; (iii) around 700^OC crystallization started, resulting in the precipitation of wollastonite. Increasing temperature improved the degree of crystallinity and densification, and a fully dense glass-ceramic material composed of wollastonite, weak anorthite, and diopside crystals plus some residual glassy phase was formed. Furthermore, it is believed that during the sintering process chrome precipitated from the glass and formed nucleation cites for the crystallization of wollastonite and diopside, and consequently induced the crystallization of the glasses as affirmed by khater *et*.al (2001).

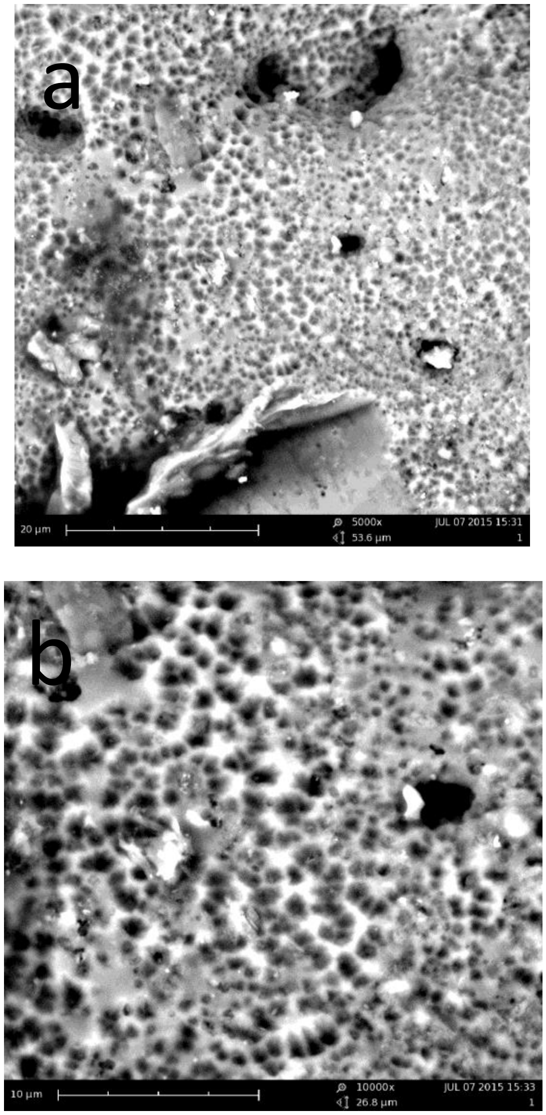

PLATEI: SEM/EDS micrographs of GC-1(-53µm, 700^{o}C), with fine texture of tiny wollastonite in residual glass matrix.

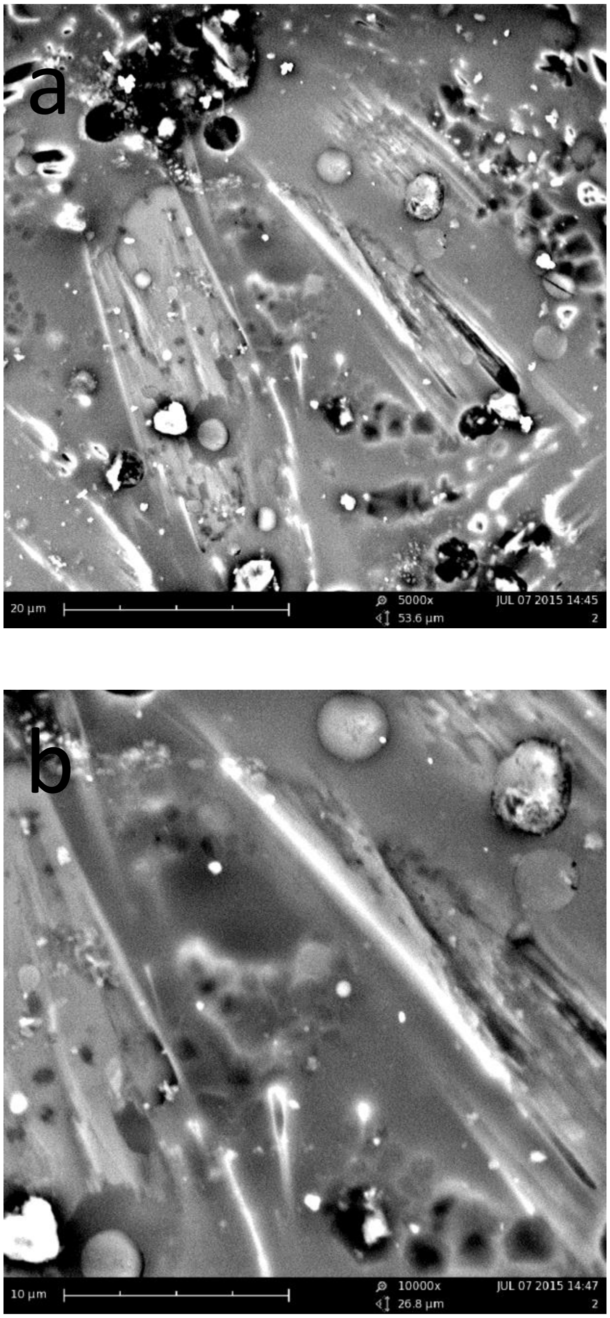

PLATEII: SEM/EDS micrographs of GC-1(-53µm, 800^{o}C): a) x5000 b) x10000, with fibrous growth of wollastonite in residual glass matrix.

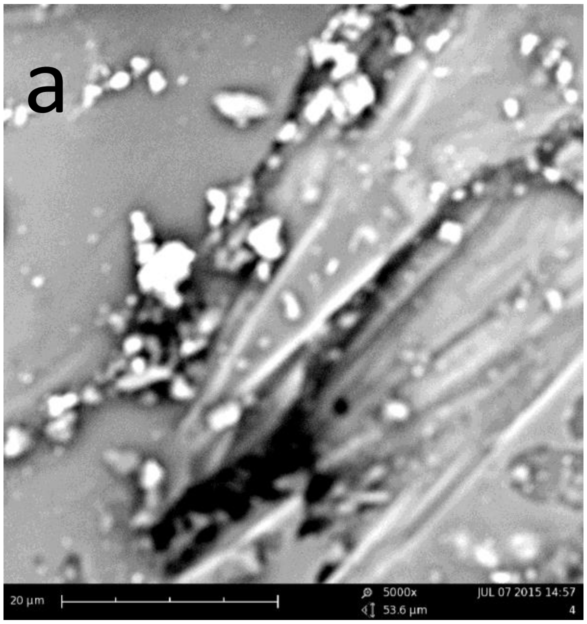

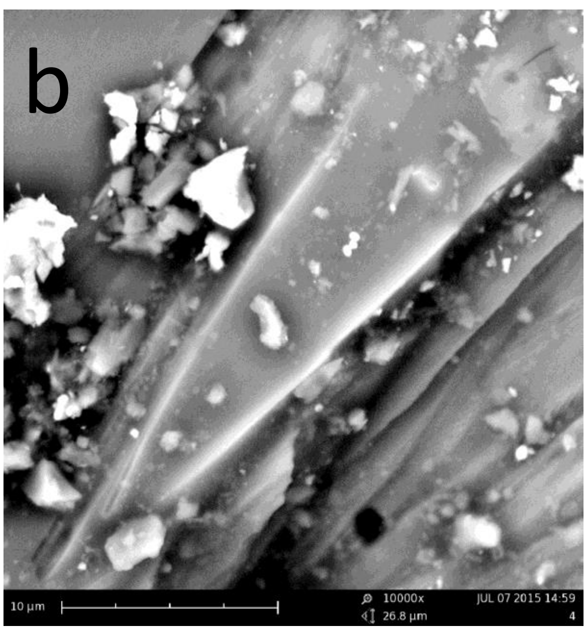

PLATEIII: SEM/EDS SEM/EDS micrographs of GC-2(-75+53µm, 700^{o}C): a) x5000 b) x10000 with fibrous growth of tiny diopside and wollastonite with appearance of tiny spherulites of anorthite

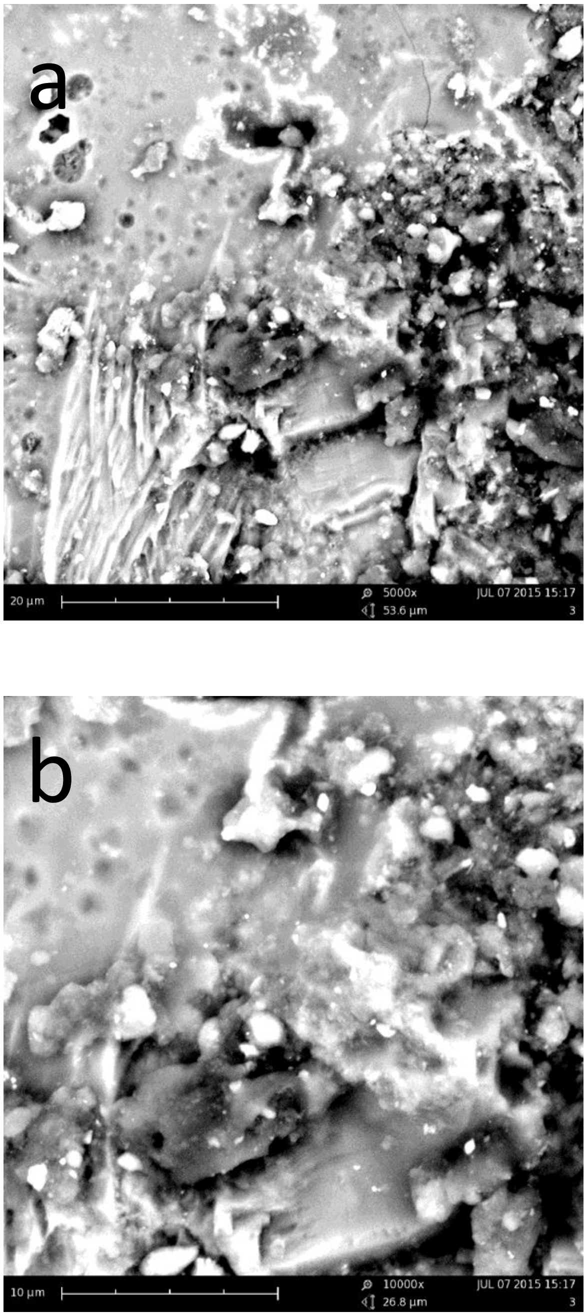

PLATEIV: SEM/EDS micrographs of GC-2(-75+53µm, 800^{o}C): a) x5000 b) x10000, showing fibrous growth of tiny diopside and wollastonite with appearance of tiny spherulites of anorthite

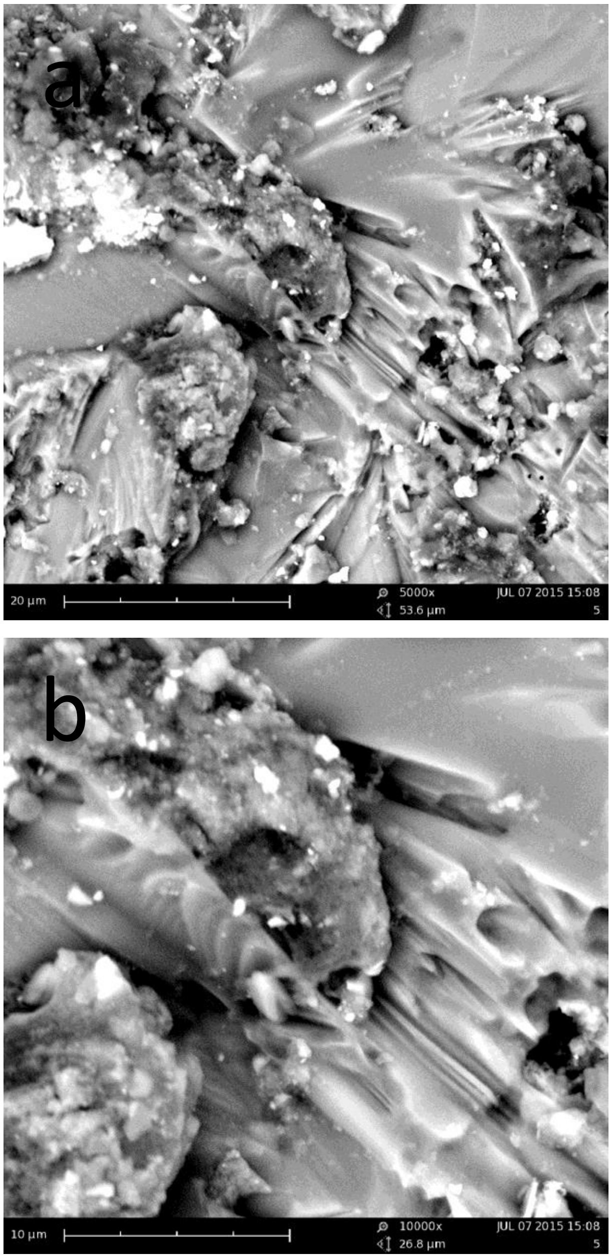

PLATEV: SEM/EDS micrographs of GC-3(-75+53µm, 800^{o}C) a) x5000 b) x10000: showing fibrous growth of tiny diopside and wollastonite with appearance of tiny spherulites of anorthite

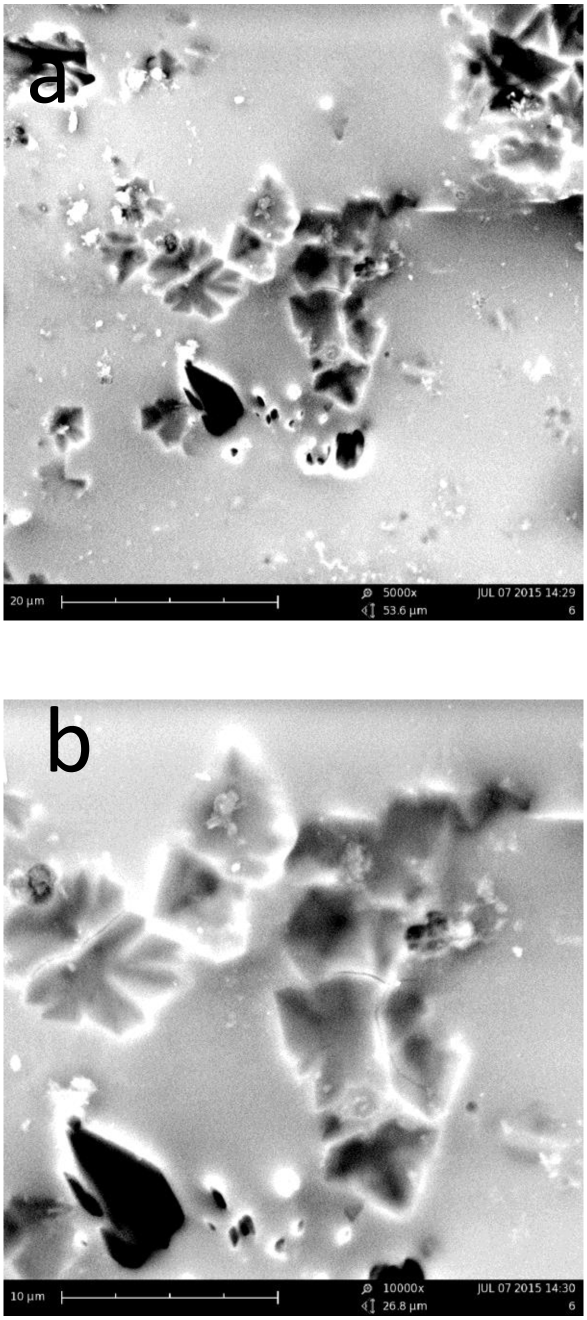

PLATEVI: SEM/EDS micrographs of GC-3(-75+53µm, 750^{o}C) a) x5000 b) x10000: showing fibrous growth of tiny diopside and wollastonite with appearance of tiny spherulites of anorthite

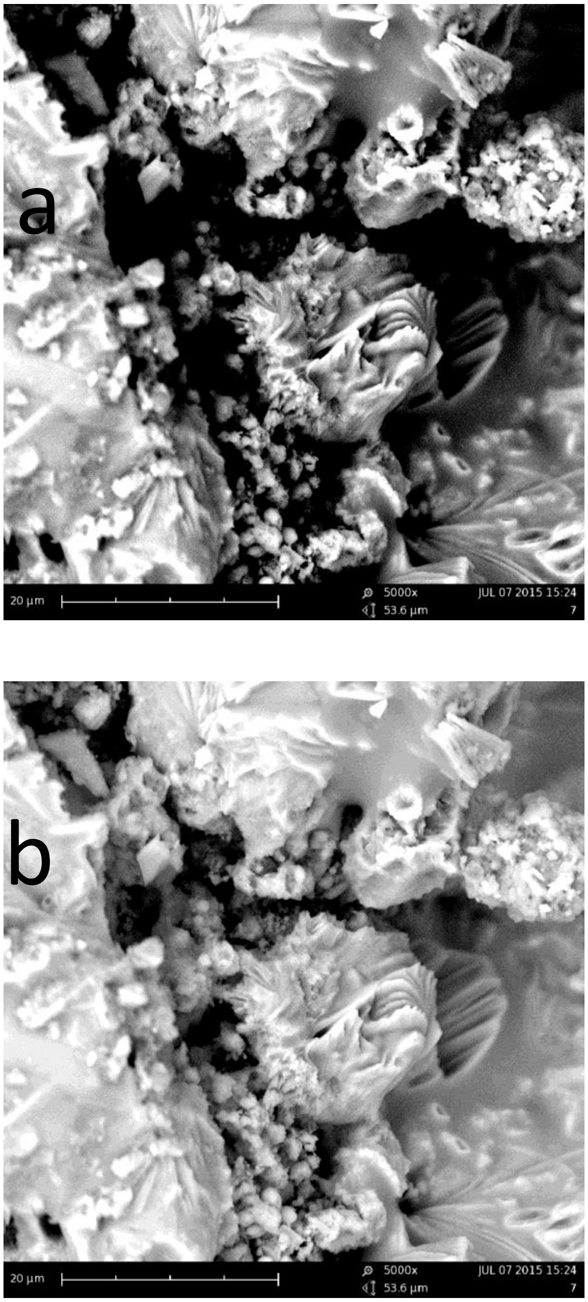

PLATEVII: SEM/EDS micrographs of GC-4(-75+53µm, 800^{o}C) a) x5000 b) x10000: showing fibrous growth of tiny diopside and wollastonite with appearance of tiny spherulites of anorthite

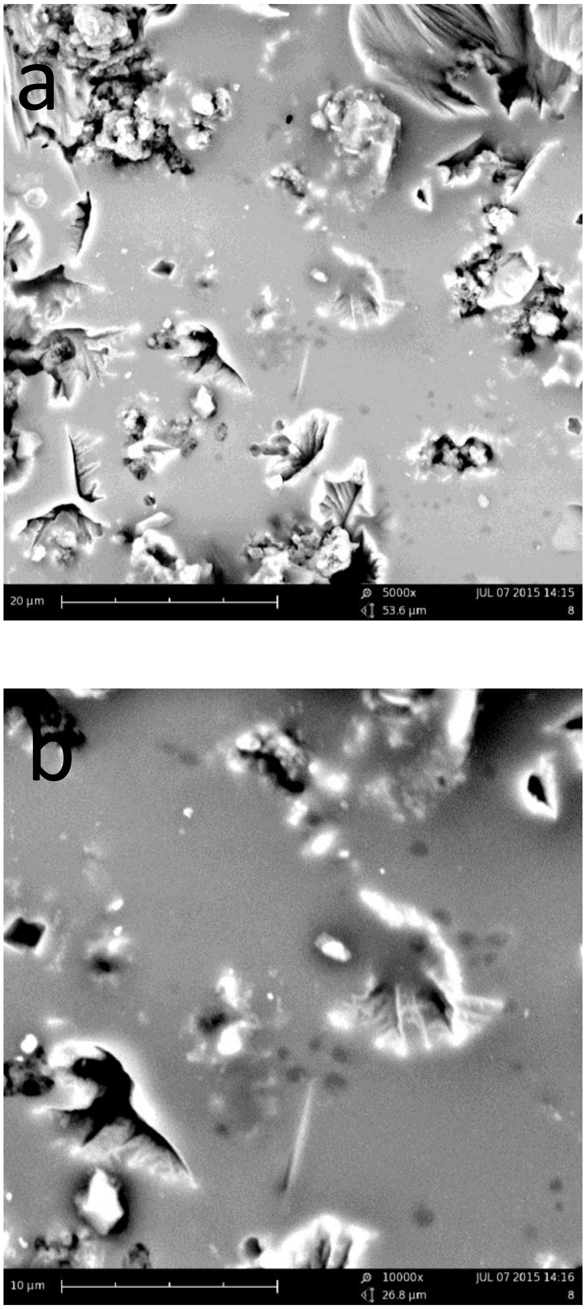

PLATEVIII: SEM/EDS micrographs of GC-4(-53µm, 750^{o}C) a) x5000 b) x10000: showing fibrous growth of tiny diopside and wollastonite with appearance of tiny spherulites of anorthite

4.2.4. Scanning Electron Microscopy

Plate's I-VIII shows the representative microstructure and morphology of the GC-1 to GC-4 sample. Two different morphologies: fine fibrous crystals assigned to wollastonite and diopside and tiny spherulites assigned to anorthite were observed. It was observed, that for GC-1 sample plates I and II wollastonite is the main phase however as the percentage of magnesite increased fibrous growth of tiny diopside and appearance of tiny spherulites of anorthite was noticed plates III-VIII. The morphology of the crystal phases present in plate 6 and 8 was quite different to the morphology observed for the other glass ceramics. The crystal phases seen in a matrix of amorphous glass were confirmed by the XRD. The EDS measurements showed clearly the presence of phosphorus although no phosphorus containing crystal phase was identified in the glass ceramic. This led to the conclusion that phosphorus must have remained in the amorphous glass. Unfortunately, it can be only a speculation that phosphorus must be present as $Ca_3(PO_4)_2$ in the glass as there is no other indication from the data presented here.

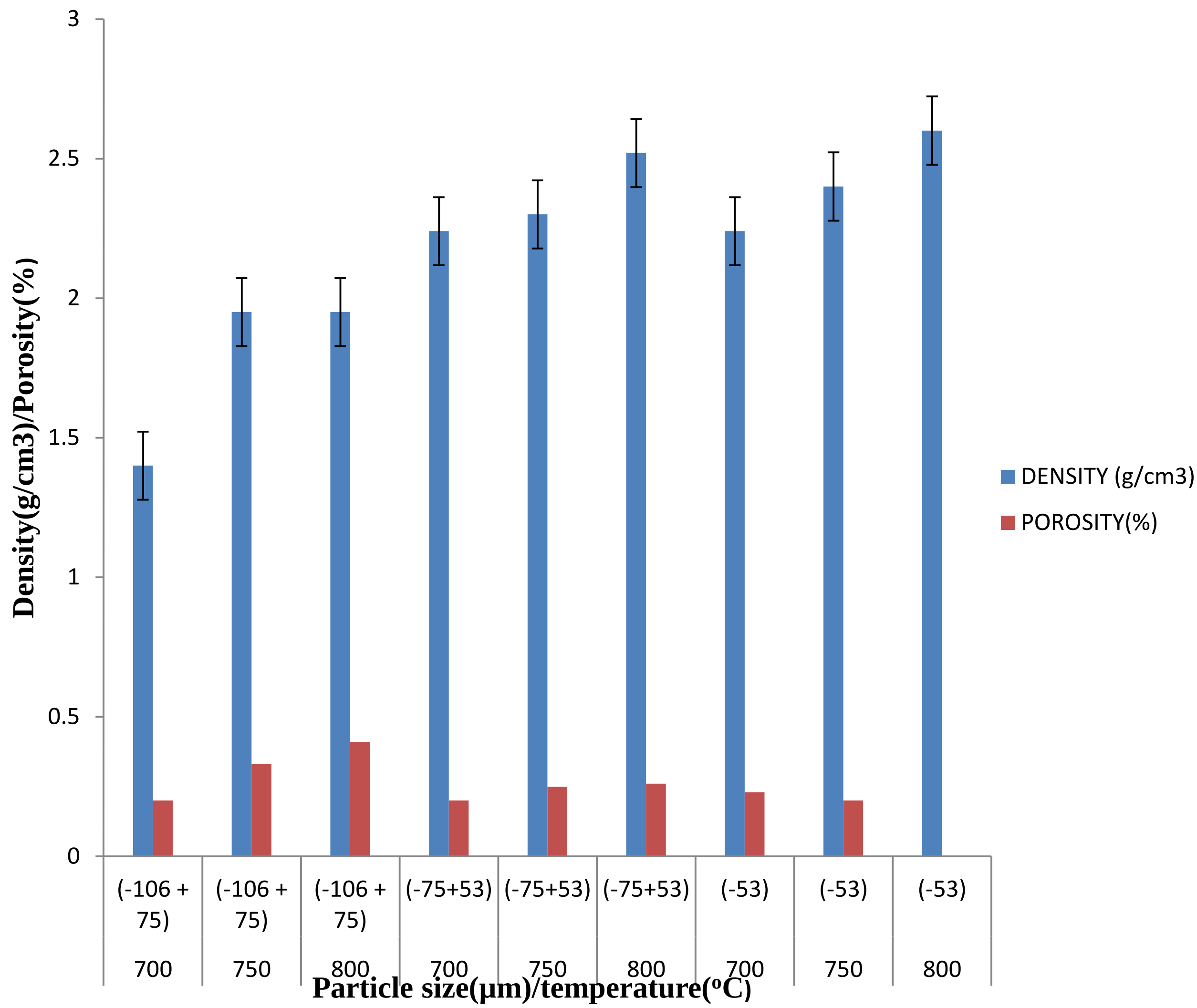

Figure4.5: Variation of density and porosity with different conditions of particle size and temperature of GC-1 samples.

\

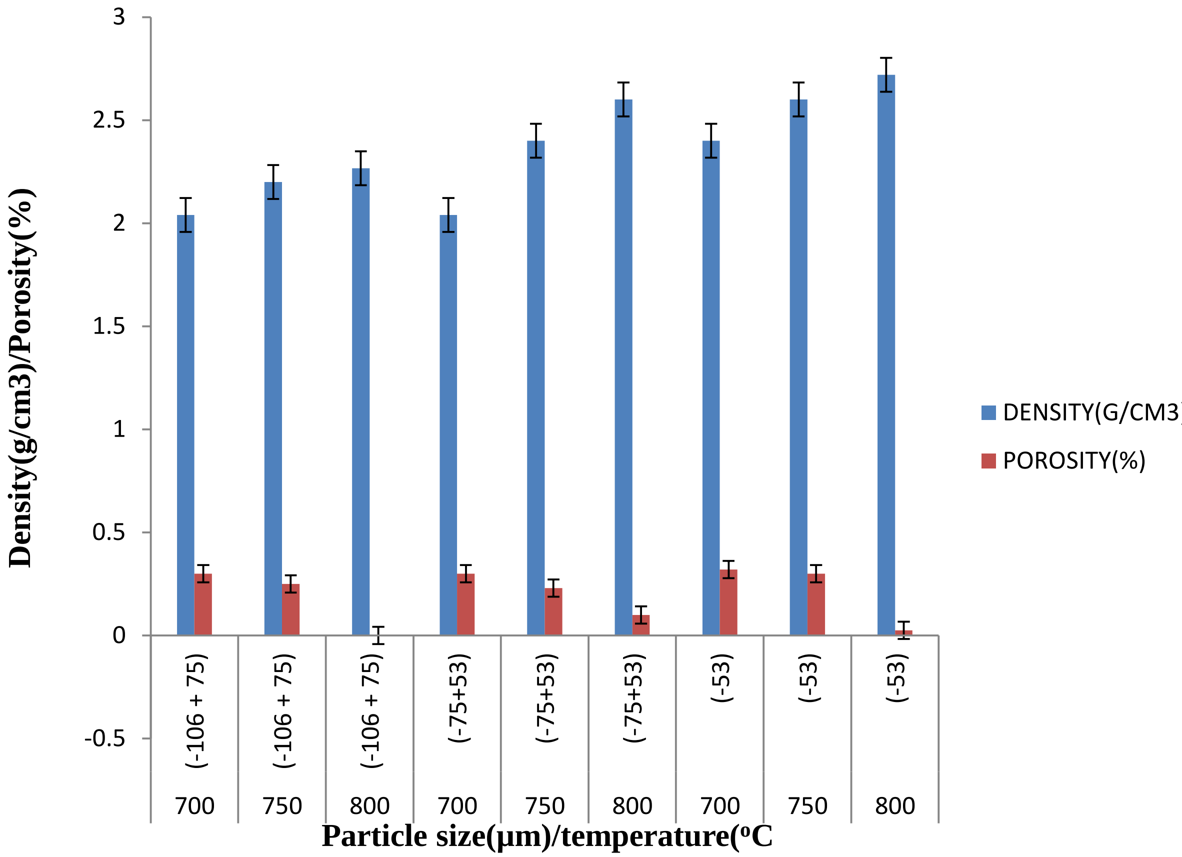

Figure4.6: Variation of density and porosity with different conditions of particle size and temperature for GC-2 samples.

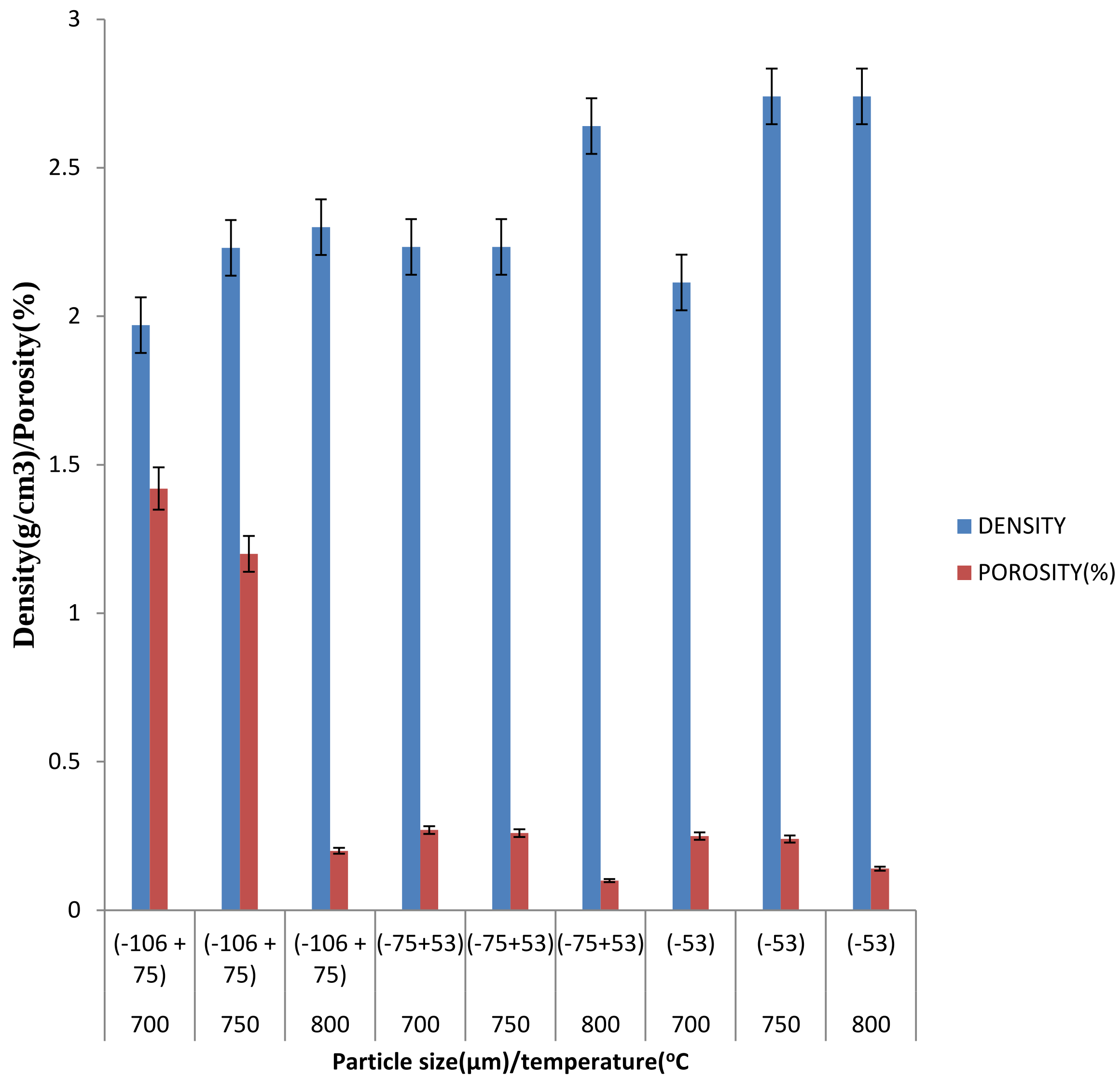

Figure4.7: Variation of density and porosity with different conditions of particle size and temperature for GC-3 samples.

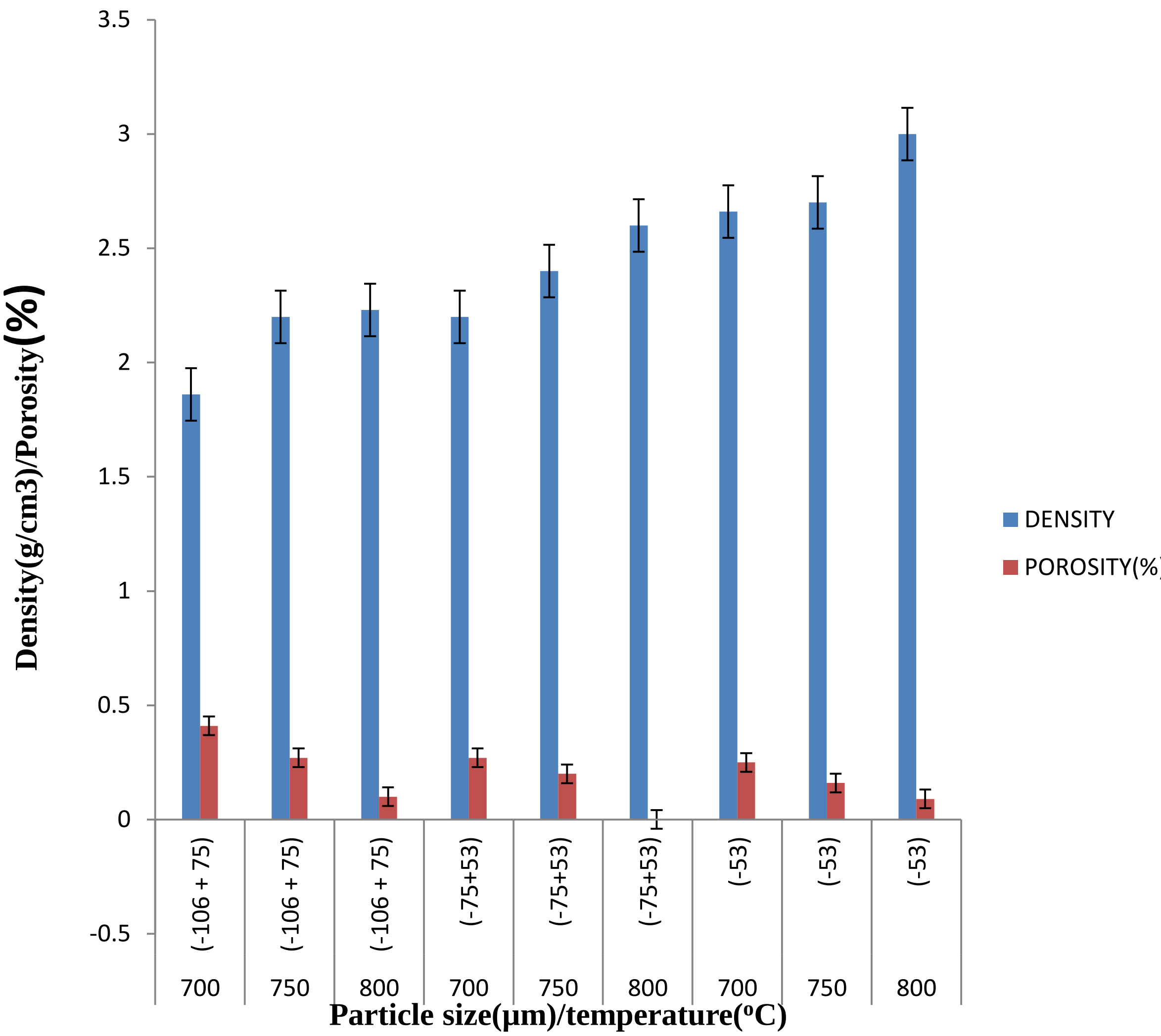

Figure4.8: Variation of density and porosity with different conditions of particle size and temperature for GC-4 samples

4.2.5 Density

Figures 4.5 to 4.8, shows variation of density with different conditions of particle size and temperature for GC-1 to GC-4. As expected, slightly higher density values were obtained for samples processed from finer particle sizes and higher temperatures. It was concluded that sinterability depended on the temperature at which the crystallization started. Therefore with increase in the crystallization temperature, the glassy phase had enough time for viscous flow which led to complete densification this agrees with Tulyaganov et.*al*, (2012). It is also observed that the maximum density of the samples was obtained at about 800 °C. The measured density values for glass ceramics were increased with increasing magnesite content. This happened because the density depended on the type of phases as well as the amount of each phase formed in the glass ceramics.

4.2.6 Porosity

Porosity or void fraction is a measure of void spaces in a material, and is the ratio of the volume of all the pores in a material to the total volume. Porosity is the result of gas entrapment in the solidifying glass ceramic materials. Figures4.5 to 4.8 shows variation of porosity with different conditions of particle size and temperature for GC-1 to GC-4. In most cases the porosity decreased with increasing temperature and decreasing particle size. This probably was because the use of fine particle sizes and high temperature promoted sintering consequently eliminating porosity.

As far as sintering is concerned, the experimental results showed that densification of sample compacts started at low temperatures (700 °C), advanced at higher temperatures, likely by viscous flow sintering, and was almost completed at 800 °C. On the other hand, crystallization started at temperatures below 700 °C and the crystallinity increases at higher temperatures, resulting in fully dense glass ceramic materials. Mirhadi and

Mehdikhani. (2012) proposed that the crystallization of diopside may cause formation of additional porosity since there is a significant difference between the density of diopisde in glassy (2.75 g/cm3) and crystal state (3.27 g/ cm3). The difference of density is negligible: in the case of wollastonite (2.87 g/cm3 and 2.92 g/cm3 for the glass and the crystals, respectively). Furthermore, SEM micrographs of samples sintered at 800^{o}C showed that the samples are without surface porosity. This means that the increase of the viscous flow at higher temperatures (800 °C) was enough to eliminate the porosity that formed due to the crystallization of diopside.

`

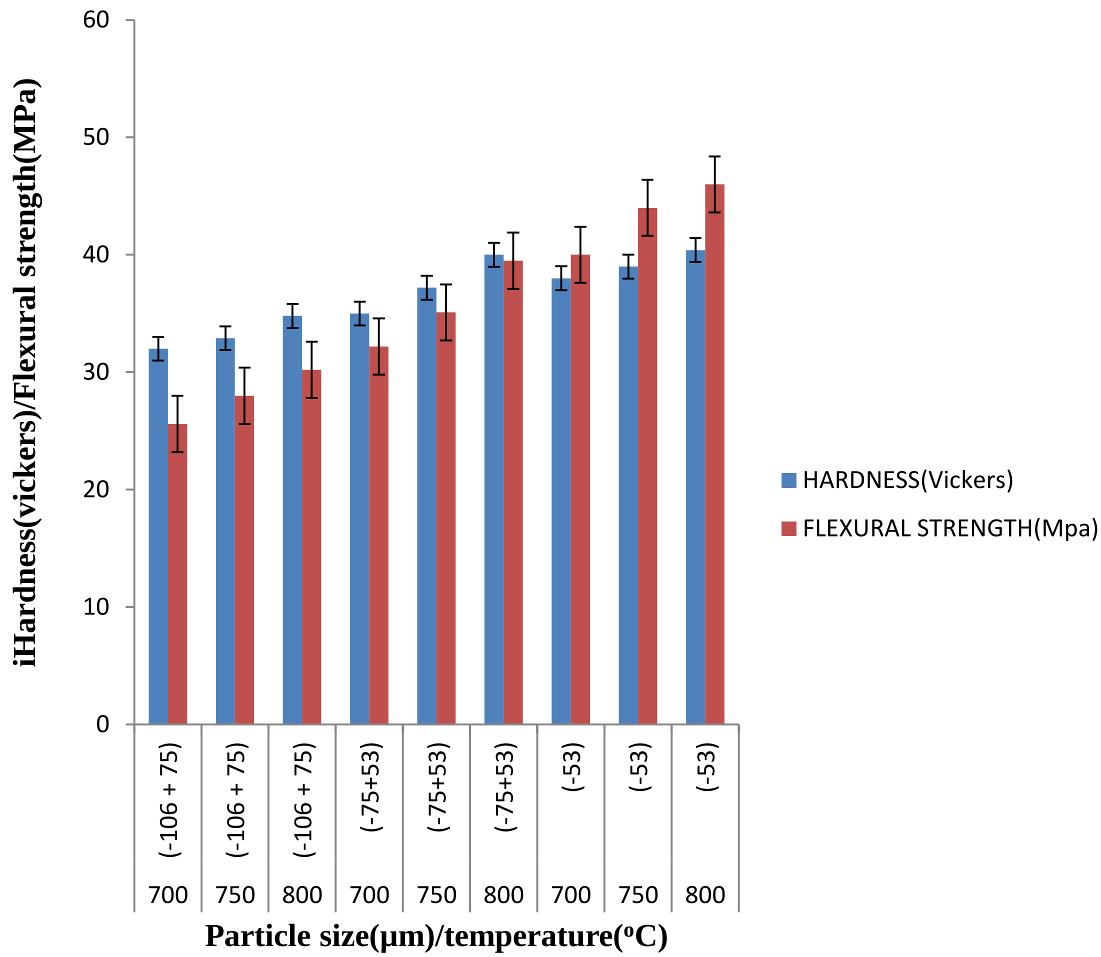

Figure4.9: Variation of hardness and flexural strength with different conditions of particle size and temperature for GC-1samples

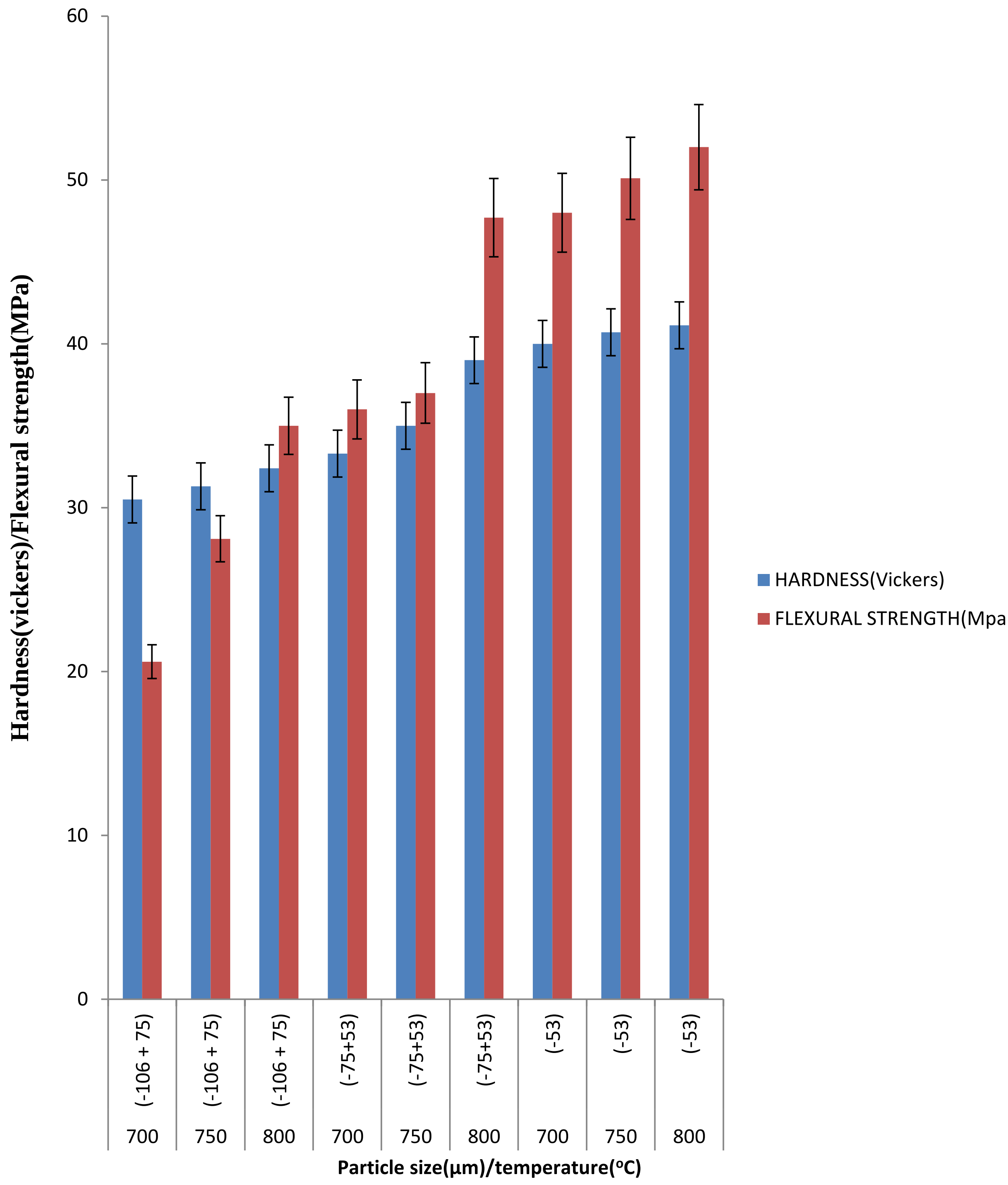

Figure4.10: Variation of hardness and flexural strength with different conditions of particle size and temperature for GC-2samples

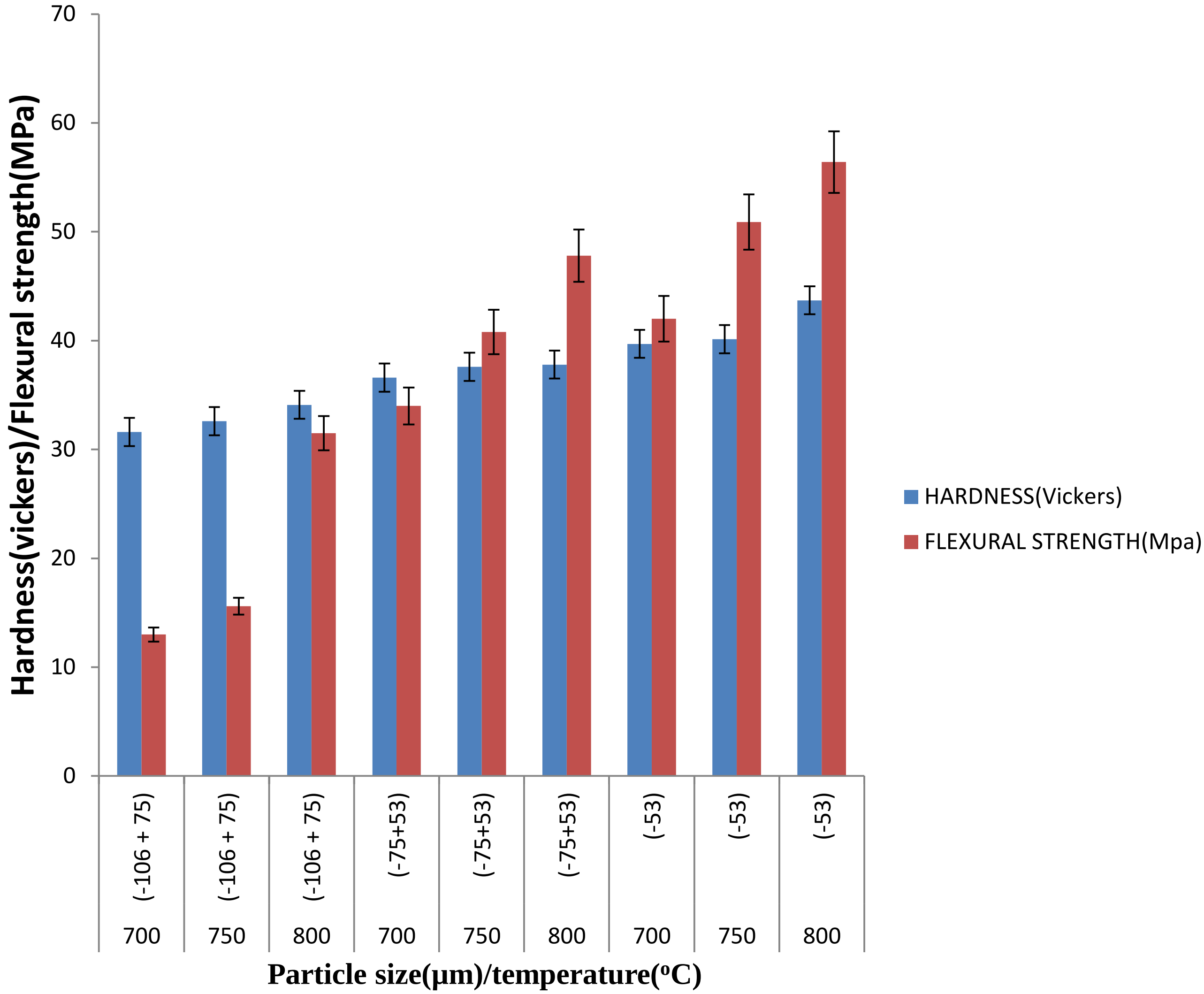

Figure4.11: Variation of hardness and flexural strength with different conditions of particle size and temperature for GC-3samples

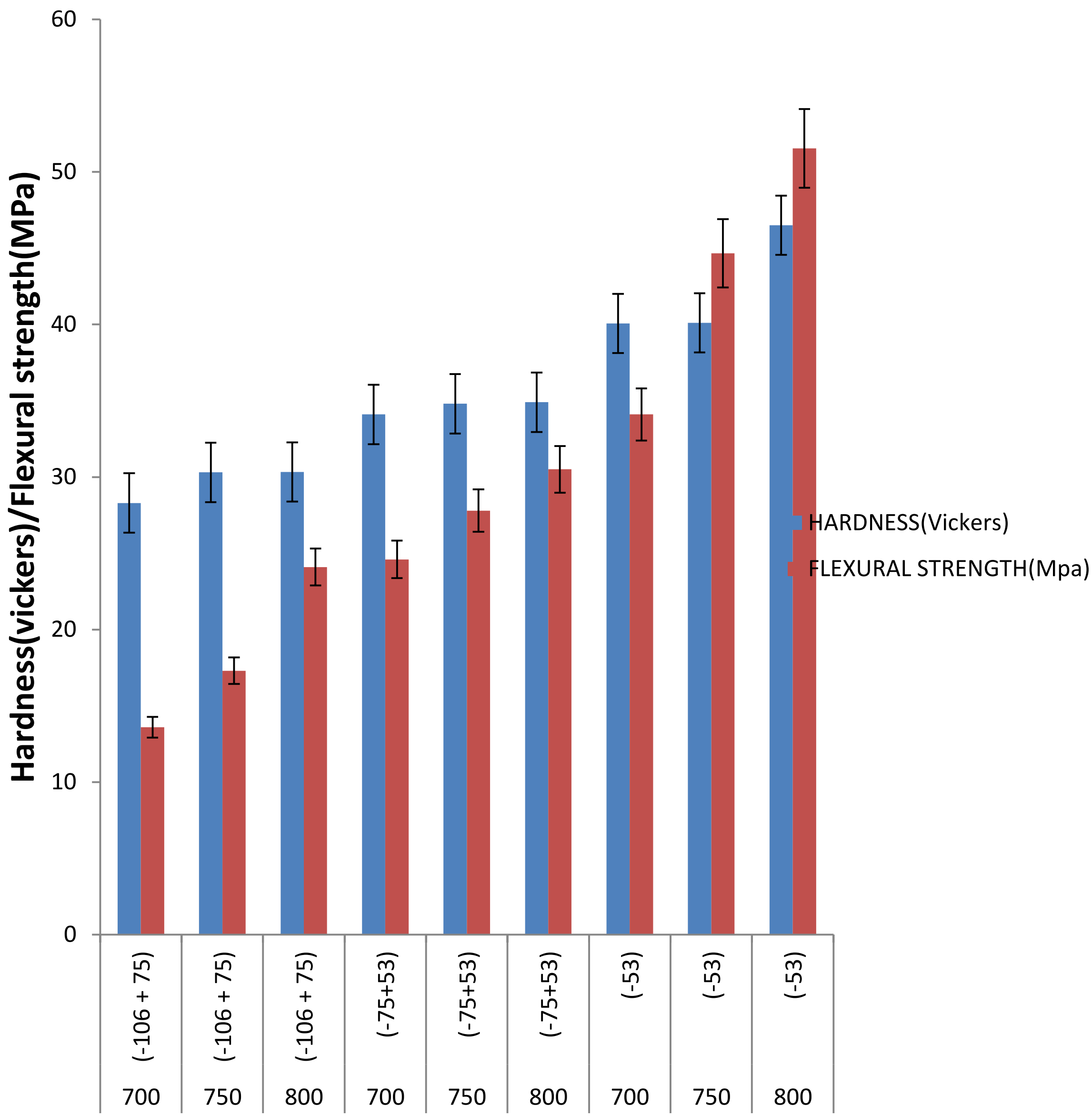

Particle size (µm)/ temperature (^{O}C)

Figure 4.12: Variation of hardness and flexural strength with different conditions of particle size (µm) and temperature (^{O}C) for GC-4sampl

4.2.7 Flexural Strength

Figures 4.9 to 4.12, show variation of flexural strength with different conditions of particle size and temperature for GC-1 to GC-4. The bending strength of the samples increased continuously up to the optimum sintering temperature, i.e. 800 °C. Perhaps the lower densities of the samples were responsible for the lower bending strength. Also the bending strength of the samples increased with increasing magnesite content, this is because compared with wollastonite, diopside belongs to monoclinic system and has better mechanical properties and chemical stability. Though both phases are inosilicates, which are well known for high strength and fracture toughness, because the unidirectional backbone of tetrahedral silica linkage often manifest itself as elongated acicular or rod like crystals that provide reinforcement to the glass ceramic . Thus, Khater et *al* (2012) proposed that diopside is a preferable crystalline phase since it results in stronger materials than glass ceramics based on wollastonite. SEM images, presented in plates, also confirmed the crystalline nature of the samples and also interlocking fibrous dendritic sheaves and spherulites which help to enhance fracture toughness as affirmed by Hölland, & Beall (2002).

4.2.8 Hardness

Figure 4.1.9 to 4.1.12, shows variation of hardness with different conditions of particle size and temperature for GC-1 to GC-4. Vickers hardness numbers increased as the diopside-anorthite eutectic or magnesite contents increase. Thus indicating the high abrasion resistance of the materials, resulting to their suitability for many applications under aggressive conditions.

CHAPTER 5

5.0 CONCLUSION AND RECOMMENDATION

5.1 Conclusion

In this research work effort has been made to develop and characterize a glass ceramic using coca cola bottle and magnesite. Based on the results obtained it was concluded that:

- ✓ Coca Cola glass bottle can be used to successfully produce glass ceramic materials possessing valuable properties.
- ✓ The resulting glass ceramic materials composed mainly of wollastonite, diopside and anorthite phases depending on composition
- ✓ Modification of the glass bottle with magnesite enhanced the properties of the obtained glass ceramics due to the precipitation of more diopside and anorthite phases.
- ✓ The density of the samples increased with increasing sintering temperature and decreasing particle size while the porosity was minimal and it decreases with increasing sintering temperature and decreasing particle size.
- ✓ The obtained glass ceramic materials possess appreciable hardness and flexural strength

5.2 Recommendation

The following are recommended for further investigation:

In the future, further work should be carried out in order to:

1 Develop a complete understanding of the crystallization mechanism of both glasses and glass ceramics.

4 The effect of time on sintering and crystallization of the glass ceramic should be investigated.

5 All batches studied should be characterized by differential scanning calorimetry to obtain the optimum nucleation temperature and activation energy of phase formation which will be calculated by Marrotta and Kissinger methods.

6 A model of the study should be developed.

REFERENCES

Ali, E.A.(2008)., *Development of low temperature glass ceramics from local raw materials*, (Doctoral Dissertation), Ahmadu Bello University, Zaria, Nigeria.

Atkinson, D. I., McMillan, P. W. (1975), *Glass-ceramics with random and oriented microstructures*, Parts I-III, *J. Mat. Sci*, 443-450.

Beall G.H. (1992), "Design and Properties of Glass-Ceramics," *Annual. Rev. Mater. Sci*., 22, 91-1 19.

Bhargava, A.K. (2005). Engineering Materials: Polymers Ceramics and Composites, PHI Learning Pvt. Ltd, India.

Boccaccini, A. R., Stumpfe, W., Taplin, D. M. R., Ponton, C. B. (1996), Densification and Crystallization of Glass Powder Compacts during Constant Heating Rate Sintering, Mater. Sci. Eng. A219, 26-31.

Boccaccini, A. R. (2001), Glass and Glass-Ceramic Matrix Composite Materials: A Review. J. Ceramic Soc Japan 109 (7) S99-S109.

Boccaccini, A. R., Rawlings, R. D. (2002), Glass and Glass-ceramic Matrix Composites: Academic Curiosity or Useful Materials? *Glass Technol. 43C,* 191-201.

Calata, J.N., (2005). Densification Behavior of Ceramic and Crystallizable Glass Materials Constrained On A Rigid Substrate (Doctoral Dissertation, Virginia Polytechnic Institute and State University)
Retrieved from http://www.freefullpdf.com

Callister, W.D. (2010). Materials science and engineering: an introduction, 8th edition, John Wiley & Sons, E-Book: Wiley Desktop Edition, (2007),

Carter, C.B. and Norton, M.G. (2007). Ceramic materials: science and engineering, Springer, EBook.

Cattell, M.J.; Chadwick, T.C.; Knowles, J.C.; Clarke, R.L. & Samarawickrama, D.Y. (2006), The nucleation and crystallization of fine grained leucite glass-ceramics for dental applications, Dent.Mater., 22,10, 925-33.

Ciacchi, F.T., Crane, K.M., and Badwal, S.P.S. (1994). Evaluation of commercial zirconia powders for solid oxide fuel cells. Solid St. Ionics, 73: 49-61.

Chowdhury, T. (2010). Ceramic Insulator, VDM Verlag, Dr. Mueller E.K, 9783639306415

David E. C. & Bruce K. Zoitos(1992). Corrosion of glass, ceramics, and ceramic superconductors: principles, testing, characterization, and applications, William Andrew.

Doremus, R.H. (1994). Glass Science, 2nd Edition, John Wiley & Sons, E-Book.

Durrani S.K.; Akhtar, J.; Ahmad, M.; M.J. Moughal M.J. (2005), *J. Mater. Sci. Technol., 21, 4,* 563-570.

Durrani S.K., Muhammad A. H,, Khalid S., Syed Z. H., Muhammad A., and Ather S. (2012). Synthesis and Sintering Studies of Magnesium Aluminum Silicate Glass Ceramic,
Retrieved fromSintering of Ceramics http://www.intechopen.com/books/sintering-of-ceramics-new emergingtechniques/synthesis-and-sintering-studies-of-magnesium-aluminum-silicate glass-ceramic.

Francis, A. A., Rawlings, R. D., Boccaccini, A. R. (2002), Glass-ceramics from Mixtures of Coal Ash and Soda-Lime Glass by the Petrurgic Method, *J. Mat. Sci, 21*, 975-978.

German, R. M.(1991), Fundamentals of Sintering in Engineered Materials Handbook ASM International, Materials Park, Ohio, Vol. 4.

Hing, P., Sinha, V., Ling, P. B. (1997), The Effect of Some Processing Parameters on the Sinterability, Microstructures and Properties of Sintered Cordierite Glass Ceramics, Journal of material processing technology, 63: pp 604-609.

Hölland, W. and Beall, G.H (2002). Glass-ceramic Technology, The American Ceramic Society, Ohio.

Khater G.A, Idris M.H. (2005) the use of Saudi kaolinitic clay for the production of glass-ceramic materials Indust. Ceram. 24: 43–49.

Khater, G. A. (2012), Preparation of glass-ceramic materials from granitic rocks waste Research, Processing and Application of Ceramics 6 (2):109–116

Koshiro, I., Mori, K., Miyamoto, H., and Nanjyo, F. (1995). 4th Symposium on SOFC In Japan edited by SOFC Society of Japan, Electrochemical Society of Japan, Tokyo, 33-40.

Kucynski G. C., Hooten N. A., and Gibson C. F.(1967). Sintering and Related Phenomena, Gordon and Breach, New York.

Kwon, O.H.(1991), Liquid Phase Sintering in Engineered Materials Handbook ASM International, Materials Park, Ohio, 4: 285-303.

Lewis M.H.(1989). Glasses and Glass-ceramics, Chapman and Hall the University of Michigan, USA.

Manfredini, T., Pellacani, G.C., and Rincón, J. M. (1997). Glass-Ceramics: Fundamentals and Applications, Publisher Mucchi, Modena, Italy.

Michael, B. (2007). Barium lanthanum silicate glass-ceramics, US Patent *7189668*.

Miller, R. and Miller, M. R. (2002). Electronics: The Easy Way, Barron's Educational Series.

Mirhadi B. and Mehdikhani B. (2012), Effect of calcium fluoride on sintering behavior of SiO2-CaO-Na2O-MgO glass-ceramic system Processing and Application of Ceramics, 6 (3): 159– 164

Montedo O. R. K., Floriano, F.J., Filho, J. O., Angoletto E., and Bernardin A.M. (2009). Sintering behavior of LZSA glass-ceramics,journal of Material. Research, 12: 197-200.

Mostaghaci, H. (1996). Applications of advanced materials in a high-tech society, Journal of Advanced ceramic materials, Trans Tech Publications.

Novaes de Oliveira A.P., Manfredini T., Leonelli C. and Peellacani, G. C.(1994). Physical Properties of Quenched Glasses in the Li2O-ZrO2-SiO2 System , Journal of American Ceramic Soceity, 79 :1092-1094.

Olevsky,E.A. and Bordia, R.(2009). Advances in Sintering Science and Technology,Vol.211,Ceramic Transactions Series, John Wiley & Sons.

Pannhorst, W. (1997). Glass ceramics: State-of-the-art, Journal of Non Crystalline Solids. 219: 198-204.

M.N. Rahaman (2003), Ceramic Processing and Sintering, 2nd ed., New York: Marcel Dekker.

Rajendran, V. (2004). Materials Science, Tata McGraw-Hill Education.

Rawlings RD, Wu JP, Boccaccini AR (2006). Glass-ceramics: Their production from wastes –A review. Journal of material science 41:733-761.

Rawlings, R. D.(1997). Production and Properties of Silceram Glass Ceramics, in Glass-Ceramic Materials. Fundamentals and Applications. Mucchi Modena, Italy.

Rice, R. and Rice, W. (2002). Ceramic Fabrication Technology, Materials engineering CRC Press, Vol 20 .

Richerson D.W., Modern Ceramic Engineering: Properties, Processing and Use in Design, 2nd ed. rev. and expanded by Marcel Dekker , New York.

Rincón, J. Ma. (1992). Principles of Nucleation and Controlled Crystallization of Glasses. Polym. Plast. Technol. Eng., 3.

Romero M., and Rincón, J. Ma., Surface and Bulk Crystallisation of Glass-ceramic in the Na_2O CaO-ZnO-PbO-Fe_2O_3-Al_2O_3-SiO_2 System Derived from a Goethite Waste**,** Journal of American Ceram. Soceity, 82: 1313-1317.

Scherer,G. W. (1977), Sintering of Low-Density Glasses. Part I. Theory, J. Am. Ceram. Soc. 60 239-243.

Scherer, G.W. (1992). Constitutive Models for Viscous Sintering in Mechanics of Granular Materials and Powder Systems, ASME, New York, 37: 1-18.

Shackelford, J. F,. and Doremus R.H. (2008). Ceramic and glass materials: structure, properties and processing, Springer.

Siligardi C., D'Arrigo M.C., Leonelli C. (2000). Sintering behavior of glass-ceramic frits, Journal of American. Ceramic. Soceity. Bull 79: 88–93.

Sintering of Ceramics – New Emerging Techniques, 278. Link: www.intechopen.com

Valenzuela, R. (2005). Magnetic Ceramics, Cambridge University Press, London.

Yuan, Q..L.; Zhang, P.; Gao, L.; Peng, H.; Ren, X. & Zhang, D.(2010). MgO-Al2O3-SiO2 Glass- Ceramic Prepared by Sol-Gel Method, Advan. Mater. Res. 92, (2010) 131 137.

Zanotto, E. D., Prado M. O. (2001), Isothermal sintering with concurrent crystallisation of monodispersed and polydispersed glass particles. Part I, Phys. Chem. Glasses 42 191-198.

Zhang,S.(2010). Effect of zinc substitution on the structure of calcium fluoro Amino Silicate Glasses and glass ceramics (MPhil thesis, University of Birmingham) Retrieved from http://www.freefullpdf.com

APPENDICES

Appendix A

Table A1: Variation of density and porosity with different conditions of particle size and temperature for GC-1 samples.

Temperature(0c)	Size Fractions (µm)	Density (G/Cm3)	Porosity (%)
700	(-106 + 75)	1.4	0.2
750	(-106 + 75)	1.95	0.33
800	(-106 + 75)	1.95	0.41
700	(-75+53)	2.24	0.2
750	(-75+53)	2.3	0.25
800	(-75+53)	2.52	0.26
700	(-53)	2.24	0.23
750	(-53)	2.4	0.2
800	(-53)	2.6	0

Table A2: Variation of density and porosity with different conditions of particle size and temperature for GC-2 samples.

Temperature	Size Fractions (µm)	Density(G/Cm3)	Porosity (%)
700	(-106 + 75)	2.04	0.3
750	(-106 + 75)	2.2	0.25
800	(-106 + 75)	2.266	0
700	(-75+53)	2.04	0.3

750	(-75+53)	2.4	0.23
800	(-75+53)	2.6	0.1
700	(-53)	2.4	0.32
750	(-53)	2.6	0.3
800	(-53)	2.72	0.025

Table A3: Variation of density and porosity with different conditions of particle size and temperature for GC-3 samples.

Temperature	Size Fractions (µm)	Density	Porosity (%)
700	(-106 + 75)	1.97	1.42
750	(-106 + 75)	2.23	1.2
800	(-106 + 75)	2.3	0.2
700	(-75+53)	2.233	0.27
750	(-75+53)	2.233	0.26
800	(-75+53)	2.64	0.1
700	(-53)	2.114	0.25
750	(-53)	2.74	0.24
800	(-53)	2.74	0.14

Table A4: Variation of density and porosity with different conditions of particle size and temperature for GC-4 samples.

Temperature	Size Fractions (µm)	Density	Porosity (%)
700	(-106 + 75)	1.86	0.41
750	(-106 + 75)	2.2	0.27
800	(-106 + 75)	2.23	0.1
700	(-75+53)	2.2	0.27
750	(-75+53)	2.4	0.2
800	(-75+53)	2.6	0
700	(-53)	2.66	0.25
750	(-53)	2.7	0.16
800	(-53)	3	0.09

Appendix B

Table B1: Variation of hardness and flexural strength with different conditions of particle size and temperature for GC-1 samples

Temperature	Size Fractions (µm)	Hardness(Vickers)	Flexural Strength(Mpa)
700	(-106 + 75)	32.9	30.2
750	(-106 + 75)	40.4	32.2
800	(-106 + 75)	41	50.8
700	(-75+53)	37.2	28
750	(-75+53)	34.8	39.5
800	(-75+53)	35	40
700	(-53)	40	25.6
750	(-53)	32	35.1
800	(-53)	45.1	58.4

Table B2: Variation of hardness and flexural strength with different conditions of particle size and temperature for GC-2 samples

Temperature	Size Fractions (µm)	Hardness(Vickers)	Flexural Strength(Mpa)
700	(-106 + 75)	32.4	36
750	(-106 + 75)	39	52
800	(-106 + 75)	40	47.7
700	(-75+53)	33.3	20.6

750	(-75+53)	35	37
800	(-75+53)	41.13	48
700	(-53)	31.3	28.1
750	(-53)	40.7	35
800	(-53)	30.5	50.1

Table B3: Variation of hardness and flexural strength with different conditions of particle size and temperature for GC-3 samples

Temperature	Size Fractions (µm)	Hardness(Vickers)	Flexural Strength(Mpa)
700	(-106 + 75)	32.4	36
750	(-106 + 75)	39	52
800	(-106 + 75)	40	47.7
700	(-75+53)	33.3	20.6
750	(-75+53)	35	37
800	(-75+53)	41.13	48
700	(-53)	31.3	28.1
750	(-53)	40.7	35
800	(-53)	30.5	50.1

Table B4: Variation of hardness and flexural strength with different conditions of particle size and temperature for GC-4 samples

Temperature	Size Fractions (µm)	Hardness(Vickers)	Flexural Strength(Mpa)
700	(-106 + 75)	40.1	27.8
750	(-106 + 75)	34.1	30.5
800	(-106 + 75)	34.9	44.67
700	(-75+53)	28.3	17.3
750	(-75+53)	30.3	34.1
800	(-75+53)	46.5	51.54
700	(-53)	40.07	24.6
750	(-53)	30.33	13.6
800	(-53)	34.8	24.1

Appendix c

Table C1: XRD Mineral Card of a) GC-1(-53µm, 700^{o}C)

Card	Chemical formula	Mineral name
25-0645	$Mg_3(Si_2\text{-}xO_5)(OH)_4\text{-}4x$	Magnesium silicate hydroxide
10-0492	KMg3(Si3Al)O10(OH)	Potassium Magnesium Aluminium silicate hydroxide
29-1016	$KMg_2Al_3(Si_3Al)O_{30}$	Potassium Magnesium Aluminium silicate
33-0664	Fe_2O_3	Iron Oxide
38-1479	Cr_2O_3	Chromium Oxide
10-0173	Al_2O_3	Aluminium oxide
13-0135	$CaO._2(Al,Mg)_2Si_4O_{10}(OH)_2.4H_2O$	Calcium Magnesium Aluminium silicate hydroxide
26-0911	$(K, H_3O)Al_2Si_3AlO_{10}(OH)_2$	Potassium Aluminium silicate hydroxide
37-1484	ZrO_2	Zirconium oxide
6-0263	$KAl_2(Si_3Al)O_{10}(OH,F)_2$	Potassium Aluminium Silicate Hydroxide
39-1425	SiO_2	Silicon oxide

Table C2: XRD Mineral Card for GC-1(-53µm, 800^oC)

Card	Chemical formula	Mineral name
10-0173	Al_2O_3	Aluminium Oxide
25-0645	$Mg_3(Si_2-xO_5)(OH)_{4-4x}$	Magnesium silicate hydroxide
5-0586	$CaCO_3$	Calcium Carbonate
10-0495	$KMg_3(Si_3Al)O_{10}(OH)_2$	Potassium Magnesium Aluminium Silicate Hydroxide
50-1606	(Mg,Fe)3Si2O5(OH)4	
37-1496	$CaSO_4$	Calcium Sulfate
23-0125	$Ca_6Si_6O_{17}(OH)_2$	Calcim Silicate hydroxide
34-0556	Mg_2SiO_4	Magnesium silicate
13-0595	$Mg_4Si_6O_{15}(OH)_{2}.{}_6H_20$	Magnesium silicate hydroxide hydrate
19-1184	$NaAlSi_3O_8$	Sodium Aluminium silicate
46-1045	SiO_2	Silicon Oxide

Table C3: XRD Mineral Card for GC-2 (-75+53µm, 700°C)

Card	Chemical formula	Mineral name
25-0645	$Mg_3(Si_2\text{-}xO_5)(OH)_{4\text{-}4x}$	Magnesium silicate hydroxide
5-0586	$CaCO_3$	Calcium Carbonate
13-0135	$CaO._2(Al,Mg)_2Si_4O_{10}(OH)_2.4H_2O$	Calcium Magnesium Aluminium silicate hydroxide
10-0495	$KMg_3(Si_3Al)O_{10}(OH)_2$	Potassium Magnesium Aluminium Silicate Hydroxide
38-1479	Cr_2O_3	Chromium Oxide
33-0664	Fe_2O_3	Iron Oxide
10-0173	Al_2O_3	Aluminium Oxide
26-0911	$(K, H_3O)Al_2Si_3AlO_{10}(OH)_2$	Potassium Aluminium silicate hydroxide
23-0125	$Ca_6Si_6O_{17}(OH)_2$	Calcim Silicate hydroxide
13-0595	$Mg_4Si_6O_{15}(OH)_2._6H_20$	Magnesium silicate hydroxide hydrate
26-0328	$CaSO_4$	Calcium Sulfate
46-1045	SiO_2	Silicon Oxide
19-1184	$NaAlSi_3O_8$	Sodium Aluminium

		silicate
17-0500	$Ca(PO_{3})_2$	Calcium Phosphate
29-0369	Ca_2SiO_4	Calcium silicate
39-1425	SiO_2	Silicon Oxide

Table C4: XRD Mineral Card for GC-2(-75+53µm, 700^oC)

Card	Chemical formula	Mineral name
27-1402	Si	Silicon
26-0911	$(K, H_3O)Al_2Si_3AlO_{10}(OH)_2$	Potassium Aluminium silicate hydroxide
31-0794	(Mg,Al)9(Si,Al)8O20(OH)10.4H2O	Magnesium Aluminium Silicate Hydroxide
23-0125	$Ca_6Si_6O_{17}(OH)_2$	Calcim Silicate hydroxide
25-0645	$Mg_3(Si_2\text{-}xO_5)(OH)_{4\text{-}4x}$	Magnesium silicate hydroxide
10-0425	Al_2O_3	Aluminium oxide
13-0135	$CaO._2(Al,Mg)_2Si_4O_{10}(OH)_2.4H_2O$	Calcium Magnesium Aluminium silicate hydroxide
17-0500	$Ca(PO_{3})_2$	Calcium Phosphate
36-0383	$(Mg,Fe)CO_3$	Iron Magnesium

		Carbonate
13-0595	$Mg_4Si_6O_{15}(OH)_2.{}_6H_20$	Magnesium silicate hydroxide hydrate
31-0966	$KAlSi_3O_8$	Potassium Aluminium Silicate
37-1496	CaSO4	Calcium Sulfate

Table C5: XRD Mineral card for GC-3(-75+53µm, 800^{o}C)

Card	Chemical formula	Mineral name
10-0357	(Na,k)(Si3Al)O8	Potassium Sodium Aluminium Silicate
13-0135	$CaO.{}_2(Al,Mg)_2Si_4O_{10}(OH)_2.4H_2O$	Calcium Magnesium Aluminium silicate hydroxide
27-0088	$CaSiO_3$	Calcium Silicate
21-1276	TiO_2	Titanium Oxide
5 – 0586	$CaCO_3$	Calcium Carbonate
29 – 1016	$KMg_2Al_3(Si_{10}Al_2)O_{30}$	Potassium Magnesium Aluminum Silicate
19 – 1184	$NaAlSi_3O_8$	Sodium Aluminum Silicate
10 – 0495	KMg_3 (Si_3Al) O_{10} $(OH)_2$	Potassium Magnesium Aluminum Silicate Hydr……

31 – 0966	$KAlSi_3O_8$	Potassium Magnesium Aluminum Silicate
16 – 0606	$Al_2Si_2O_5(OH)_4$	Aluminum Silicate Hydroxide
33 – 0311	$CaSO_4 . 2H_2O$	Calcium Sulfate Hydrate
39 – 1425	SiO_2	Silicon Oxide

Table C6: XRD Mineral card for GC-3(-75+53µm, 750^oC)

Card	Chemical formula	Mineral name
38-1479	Cr_2O_3	Chromium Oxide
25 - 0645	$Mg_3(Si_2\text{-}xO_5)(OH)_{4\text{-}4x}$	Magnesium silicate hydroxide
10 – 0495	$KMg_3(Si_3Al)O_{10}(OH)_2$	Potassium Magnesium Aluminium Silicate
46 - 1045	SiO_2	Silicon Oxide
36 – 0426	$CaMg(CO_3)$	Calcium Magnesium Carbonate
29 – 1016	$KMg_2Al_3(Si_3Al)O_{30}$	Potassium Magnesium Aluminium silicate
19 – 1184	NaAlSi3O8	Sodium Aluminum Silicate
26 – 0911	$(K, H_3O)Al_2Si_3AlO_{10}(OH)_2$	Potassium Aluminium silicate hydroxide
6 – 0263	$KAl_2(Si_3Al)O_{10}(OH,F)_2$	Potassium Aluminium Silicate

		Hydroxide
39 – 1425	SiO_2	Silicon Oxide
44 – 0517	$CaSO_3$	Calcium Sulfite

Table C7: XRD Mineral card for GC-4 (-75+53µm, 800^oC)

Card	Chemical formula	Mineral name
10 – 0173	Al_2O_3	Aluminium oxide
5 – 0586	$CaCO_3$	Calcium Carbonate
33 – 0664	Fe_2O_3	Iron Oxide
44 – 1472	$MnCO_3$	Manganese Carbonate
36 – 0383	$(Mg,Fe)CO_3$	Iron Magnesium Carbonate
25 – 0645	$Mg_3(Si_2\text{-}xO_5)(OH)_{4-4x}$	Magnesium silicate hydroxide
34 – 0556	Mg_2SiO_4	Magnesium silicate
39 – 1425	SiO_2	Silicon Oxide
35 – 0463	$LiAlSi_4O_{10}$	Lithium Aluminium Silicate
38 – 1479	Cr_2O_3	Chromium Oxide
6 – 0263	$KAl_2(Si_3Al)O_{10}(OH,F)_2$	Potassium Aluminium Silicate Hydroxide
17 – 0500	$Ca(PO_3)_2$	Calcium Phosphate
5 – 0378	$BaCO_3$	Barium Carbonate

Table C8: XRD Mineral card for GC-4(-53µm, 750^{o}C)

Card	Chemical formula	Mineral name
5 – 0586	$CaCO_3$	Calcium Carbonate
10 – 0173	Al_2O_3	Aluminium oxide
38 – 1479	Cr_2O_3	Chromium Oxide
49 – 1057	K-Mg-Al-SiO_2-H_2O	Potassium Magnesium Aluminium Silicate
44 – 1472	$MnCO_3$	Manganese Carbonate
13 – 0135	$CaO._2(Al,Mg)_2Si_4O_{10}(OH)_2.4H_2O$	Calcium Magnesium Aluminium silicate hydroxide
29 – 1016	$KMg_2Al_3(Si_3Al)O_{30}$	Potassium Magnesium Aluminium silicate
29 – 1488	$Al_2Si_2O_5(OH)_4$	Aluminium Silicate Hydroxide
13 – 0595	$Mg_4Si_6O_{15}(OH)_2.6H_2O$	Magnesium Silicate hydroxide hydrate
46 – 1045	SiO_2	Silicon Oxide
5 – 0378	$BaCO_3$	Barium Carbonate